Universidade de Aveiro
2016
Departamento de Engenharia Mecânica

POOJA VARDHINI NATESAN

Fabricação e Caraterizaçao de Biomateriais de Policaprolactona/óxido de Grafeno Para Aplicações em Engenharia de Tecidos

Fabrication and Characterization of Polycaprolactone/ Graphene Oxide Electrospun Scaffolds for Tissue Engineering Applications

Universidade de Aveiro
2016
Departamento de Engenharia Mecânica

POOJA VARDHINI NATESAN

Fabricação e Caraterizaçao de Biomateriais de Policaprolactona/óxido de Grafeno Para Aplicações em Engenharia de Tecidos

Fabrication and Characterization of Polycaprolactone/ Graphene Oxide Electrospun Scaffolds for Tissue Engineering Applications

Dissertação apresentada à Universidade de Aveiro para cumprimento dos requisitos necessários à obtenção do grau de Mestre em Engenharia Mecânica, realizada sob a orientação científica da Doutora Paula Alexandrina de Aguiar Pereira Marques, Equiparada a Investigadora Principal do Departamento de Engenharia Mecânica da Universidade de Aveiro e coorientação científica do Doutor António Manuel Godinho Completo, Professor Auxiliar c/ Agregação do Departamento de Engenharia Mecânica da Universidade de Aveiro

FINANCIAL SUPPORT:

ERASMUS MUNDUS SVAAGATA SCHOLARSHIP

IF/00917/2013/CP1162/CT0016

PTDC/EMS-TEC/3263/2014

This thesis is dedicated to my beloved parents and grandparents

For their endless love, support and encouragement

O Júri

Presidente	Professor Doutor Alfredo Manuel Balacó de Morais Professor Associado, Universidade de Aveiro
Vogal - Arguente Principal	Professora Doutora Maria Helena Figueira Vaz Fernandes Professora Associado, Universidade de Aveiro
Vogal - Orientador	Doutora Paula Alexandrina de Aguiar Pereira Marques Equiparada a Investigadora Principal, Universidade de Aveiro

Acknowlegement

I would like to express my deep sense of gratitude to my Supervisor, Dr.Paula Alexandrina de Aguiar Pereira Marques, Principal Investigator, Department of Mechanical Engineering, University of Aveiro for providing her expert guidance, constant encouragement, constructive criticism and all the necessary facilities.

I wish to thank my Co-Supervisor, Dr.António Manuel Godinho Completo, Assistant Professor, Department of Mechanical Engineering, University of Aveiro for his beneficial suggestions which were vital to improve the quality of this project.

I am extremely grateful to the Erasmus Mundus Action 2 Svaagata Programme for providing me this unique opportunity to carry out the final semester of my Undergraduation as an Exchange student at the University of Aveiro with financial support.

I extend my thanks to all my fellow labmates for their help throughout the research work.

Finally, I am deeply indebted to my parents for providing their unconditional love and support which greatly helped me to complete this project successfully.

Palavras-Chave Engenharia de tecidos, Fibras por electrofiação, Policaprolactona, óxido de grafeno

Resumo

A recente evolução científica no campo da engenharia de tecidos (TE) criou oportunidades únicas para fabricar tecidos de substituição de órgãos artificiais em laboratório a partir de combinações de matrizes extracelulares (andaimes), células e moléculas biologicamente ativas. adicionalmente, a formulação de compósitos poliméricos reforçados com cargas nanométricas como o óxido de grafeno (GO) mostrou ser possível uma grande melhoria de várias propriedades destes compósitos em relação aos polímeros simples. No presente estudo, matrizes fibrosas de policaprolactona (PCL) e de PCL-GO foram preparadas através de eletrofiação sob diferentes condições. Foi analisado o efeito de vários parâmetros de electrofiação tais como, peso molecular do polímero, solventes, concentração, caudal, tensão e distância de trabalho, sobre a morfologia das fibras eletrofiado. A incorporação de GO nas fibras de PCL alterou a morfologia, química de superfície e as propriedades mecânicas das fibras de PCL compósitos, o que foi comprovado por meio de várias técnicas de caracterização. As matrizes fibrosas de PCL-GO com a concentração de GO de 0,1% em peso demonstraram ser a combinação mais interessante para estudos futuros em TE.

Keywords Tissue engineering, Scaffolds, Polycaprolactone, Graphene Oxide

Abstract

Scientific advancements in the field of tissue engineering (TE) have created unique opportunities to fabricate artificial tissue or organ replacement components in the laboratory from combinations of engineered extracellular matrices (scaffolds), cells and biologically active molecules. Polymer composites reinforced with nanosized graphene oxide (GO) fillers have shown large improvement of various properties over the pristine polymers. In the present study, polycaprolactone (PCL) and PCL-GO fibres were prepared through electrospinning under different conditions. The effect of several electrospinning parameters (polymer molecular weight, solvent system, concentration, flow rate, voltage and working distance) on the morphology of the electrospun fibres was investigated. The GO nanosheets were successfully incorporated into the PCL fibres and the changes in the morphology, surface chemistry and mechanical properties were analyzed through various characterization techniques. The PCL-GO electrospun fibres with GO concentration of 0.1 wt% was found to be the most attractive combination which can be utilized for future TE applications.

TABLE OF CONTENTS

CHAPTER NO. **TITLE** **PAGE NO.**

LIST OF TABLES

LIST OF FIGURES

FIGURE NO.	TITLE	PAGE NO.

LIST OF SYMBOLS AND ABBREVIATIONS

2EEA	-	2-Ethoxyethyl Acetate
2EH	-	2-Ethyl Hexanol
a.u.	-	Absorbance Units
AA	-	Acetic Acid
C-H	-	Aliphatic
AGO	-	Amine-Functionalized Graphene Oxide
θ	-	Angle
~	-	Approximately
AFM	-	Atomic Force Microscopy
BM	-	Benzenemethanol
BB	-	Bromobenzene
BE	-	Butoxyethanol
C-C	-	Carbon-Carbon
CNTs	-	Carbon Nanotubes
C-O	-	Carbon-Oxygen
C=O	-	Carbonyl
COOH	-	Carboxyl
cm	-	Centimetre
CCD	-	Charge Coupled Device
CVD	-	Chemical Vapour Deposition
$CHCl_3$	-	Chloroform
cts	-	Counts
c_e	-	Critical Minimum Concentration
CB	-	Cyclobenzene
CHL	-	Cyclohexanol
CHN	-	Cyclohexanone
°	-	Degree
°C	-	Degree Celsius
°/min	-	Degree per Minute
DNA	-	Deoxyribonucleic Acid
DAA	-	Diacetone Alcohol
DCB	-	Dichlorobenzene
DCM	-	Dichloromethane

DEC	-	Diethyl Carbonate
DEG	-	Di(ethylene glycol)
DEE	-	Diethyl Ether
DMSO	-	Dimethylsulphoxide
DPG	-	Di(propylene glycol)
DC	-	Direct Current
f_d	-	Dispersion Forces
DLS	-	Dynamic Light Scattering
EDS	-	Energy Dispersive Spectroscopy
C-O-C	-	Epoxy
EtOH	-	Ethanol
EtAc	-	Ethyl Acetate
$\eta_{extensional}$	-	Extensional Viscosity
ECM	-	Extracellular Matrix
FDA	-	Food and Drug Administration
FA	-	Formic Acid
FTIR	-	Fourier Transform Infrared Spectroscopy
fGO	-	Functionalized Graphene Oxide
G	-	Gauge
Ge	-	Germanium
T_g	-	Glass Transition Temperature
GO	-	Graphene Oxide
GOQDs	-	Graphene Oxide Quantum Dots
He-Ne	-	Helium-Neon
hMSCs	-	Human Mesenchymal Stem Cells
f_H	-	Hydrogen Bonding
OH	-	Hydroxyl
HPU	-	Hyperbranched Polyurethane
Fe_3O_4	-	Iron(II,III) Oxide
K	-	Kelvin
kDa	-	Kilo Dalton
kV	-	Kilo Volt
Li	-	Lithium
CH_3OH/MeOH	-	Methanol

MeAc	-	Methyl Acetate
CH_2	-	Methylene
mg/mL	-	Milligram per Millilitre
mL/h	-	Millilitre per Hour
mm	-	Millimetre
mm/min	-	Millimetre per Minute
mW	-	Milli Watt
nm	-	Nanometre
BuOH	-	n-Butanol
BuAc	-	n-Butyl Acetate
Nd:YAG	-	Neodymium-doped Yttrium Aluminium Garnet
NSCs	-	Neural Stem Cells
Ni	-	Nickel
HNO_3	-	Nitric Acid
DMAc	-	N,N-Dimethylacetamide
DMF	-	N,N-Dimethylformamide
NIBS	-	Non-Invasive Back Scatter
PrOH	-	n-Propanol
M_n	-	Number Average Molecular Weight
DCE	-	o-Dichloroethane
fGO	-	PCL-Functionalized Graphene Oxide
%	-	Percent
π	-	Pi
f_p	-	Polar Forces
PCL	-	Polycaprolactone
PEI	-	Poly(ethylenimine)
PGA	-	Polyglycolic Acid
PLGA	-	Poly(lactic-co-glycolic acid)
PLLA	-	Poly(L-lactic acid)
PHB	-	Poly((R)-3-hydroxybutyric acid)
PU	-	Polyurethane
KBr	-	Potassium Bromide
$KClO_3$	-	Potassium Chlorate
$KMnO_4$	-	Potassium Permanganate
PG	-	Propylene Glycol

P	-	Pyridine
RGO	-	Reduced Graphene Oxide
ROP	-	Ring Opening Polymerization
rpm	-	Revolutions per Minute
SEM	-	Scanning Electron Microscope
η_{shear}	-	Shear Viscosity
S/cm	-	Siemen per Centimetre
sGO	-	Silylated Graphite Oxide
SWCNTs	-	Single Walled Carbon Nanotubes
$NaNO_2$	-	Sodium Nitrite
H_2SO_4	-	Sulphuric Acid
TPa	-	Tera Pascal
TCE	-	Tetrachloroethylene
THF	-	Tetrahydrofuran
TEGO	-	Thermally Exfoliated Graphene Oxide
TRG	-	Thermally Reduced Graphene
3D	-	Three Dimensional
TE	-	Tissue Engineering
2D	-	Two Dimensional
UCB	-	Umbilical Cord Blood
v/v	-	Volume/Volume
cm^{-1}	-	Wave Number
wt	-	Weight
w/v	-	Weight/Volume
XRD	-	X-Ray Diffraction

CHAPTER 1

INTRODUCTION

1.1 SCAFFOLDS

Tissue engineering (TE) is an interdisciplinary field involving the knowledge from biology, chemistry, physics, engineering, materials science, life science and clinical science. The inability to fulfil the growing demand for tissues and organs for transplantation by the autogenic (from the host) and allogenic (from the same species) sources due to donor site morbidity and limited availability has led to the rapid development of TE as an alternative approach (Greenwald et al 2006). It involves the fabrication of biological substitutes that restore, maintain or improve the functions of the tissues or a whole organ using a combination of cells, biomaterials, bioactive molecules, suitable biochemical and physico-chemical factors. The extracellular matrix (ECM) is the optimized milieu that nature has provided in order to maintain homeostasis and to direct tissue development. Hence, a great effort has been made to mimic the ECM so as to guide the morphogenesis in TE and repair.

TE makes use of scaffolds to provide support for the cells to regenerate new ECM which has been destroyed by disease, injury or congenital defects without stimulating any immune response. Scaffolds are central components of many TE strategies because they provide an architectural context in which the interactions of the ECM, cells and growth factors combine to develop regenerative niches. There is a significant challenge in the design and manufacture of the scaffolds as they possess both a highly porous structure and the ability to control the release kinetics of the growth factors over the period of tissue regeneration. Specific cells from a patient are isolated through a small biopsy in order to grow them on a 3D scaffold under controlled culture conditions. Subsequently, the construct is delivered to the desired site in the patient's body with the aim to direct new tissue formation into the scaffold which gets degraded over time as shown in Figure 1. The use of isolated cells or tissue-inducing substances is considered when the defects are small and well contained. An alternative approach is to implant scaffolds for

tissue ingrowth directly in vivo with the purpose to stimulate and direct tissue formation in situ. The advantage of this approach is the reduced number of operations resulting in a shorter recovery time for the patient (Rezwan et al 2006).

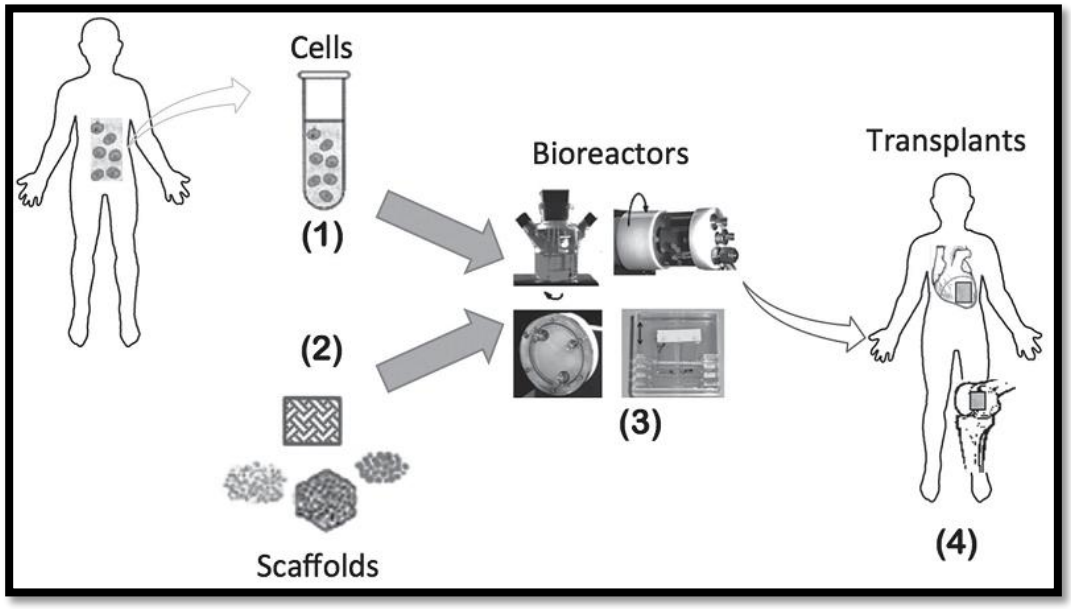

Figure 1 Scaffold-based Tissue Engineering (Freed and Guilak 2007)

(1) Cells are isolated from the patient or derived from established stem cell cultures

(2) A scaffold is constructed with the correct physical, mechanical, chemical and structural cues to encourage the development of cells into tissues

(3) Cells are seeded onto the scaffold in vitro and transferred into a bioreactor. The scaffold encourages cell proliferation and/or differentiation, the construct is incubated until the nascent tissue is ready for implantation

(4) The tissue-engineered scaffold with cells is re-implanted into the patient to develop into an integrated tissue

The scaffolds used in TE applications should possess the following characteristics:

- Three-dimensional templates with high porosity which are critical in ensuring spatially uniform cell distribution, survival, proliferation and migration in vitro,

neovascularization from surrounding tissues in vivo and flow transport of nutrients, gases and metabolic wastes

- High internal surface area to volume ratios which are essential to accommodate the large numbers of cells required to replace or restore the functions of tissues or organs
- Biocompatible, bioresorbable, erodable, non-toxic, non-mutagenic, non-antigenic, non-carcinogenic and non-teratogenic
- Mechanical properties matching those of the tissues at the implantation site which are sufficient to shield the cells from the damaging compressive or tensile forces without inhibiting appropriate biomechanical cues
- Synchronization of polymer degradation at a controllable rate with the replacement by natural tissues produced from the cells and easy excretion of the degradation products by metabolic pathways
- Easy sterilization to prevent infections

1.1.1 Polycaprolactone Scaffolds

Polymers (macromolecules) are the primary materials for scaffolds in various TE applications as they do not dissolve or melt under in vitro tissue culture conditions or when implanted in vivo (Ma 2004). They can be divided into two main categories:

- Natural polymers including alginate, collagen, hyaluronan, chitosan and gelatin
- Synthetic polymers including polyesters like polycaprolactone, polyaminoamides, polyacrylates and their copolymers and blends

Polycaprolactone (PCL) was one of the polymers synthesized by the Carothers group in the early 1930s. It became commercially available following the efforts to identify synthetic polymers that could be degraded by micro-organisms (Huang 1985). It is a semi-crystalline, linear, aliphatic and easily obtainable polyester having a low melting point of 60°C and a glass transition temperature of -60°C. PCL is prepared by the Ring Opening Polymerization (ROP) of a relatively cheap, cyclic monomeric unit, ε-caprolactone using a variety of anionic, cationic

and co-ordination catalysts such as stannous octoate or via free radical ROP of 2-methylene-1-3-dioxepane (Pitt 1990) as illustrated in Figure 2.

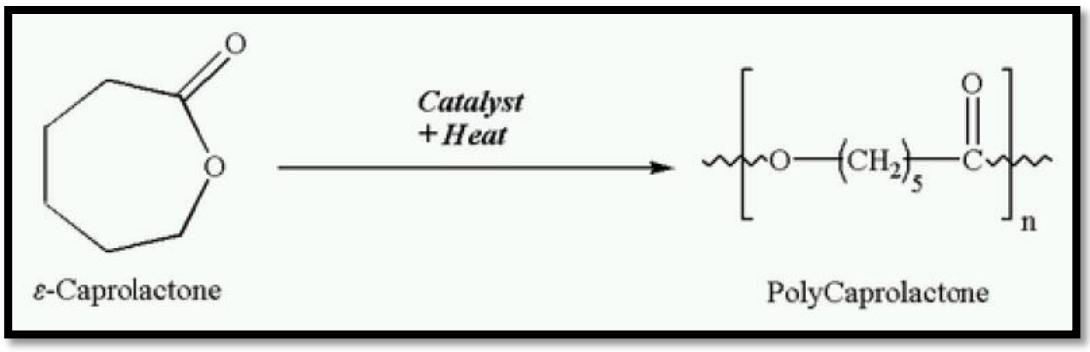

Figure 2 Synthesis of PCL (Sravanthi 2009)

PCL has excellent physical properties such as elasticity, softness and lightness but, it is strong enough to be handled. It has good resistance to water, chlorine, solvents and oil. It is well known for its slow biodegradability (>24 months to lose total mass), high biocompatibility, excellent electrospinnability, low toxicity, good drug permeability, enhanced solubility in organic solvents, exceptional blend-compatibility, processability at low temperatures, tailorable degradation kinetics, high chemical and thermal stability, non-toxic degradation byproducts, high elongation, ease of bio-functionalisation, hard and soft tissue compatibility, proven cytocompatibility and is also approved by the Food and Drug Administration (FDA). Unlike commonly used biodegradable polymers such as poly(D,L-lactic-co-glycolic acid), PCL does not produce a local acidic environment as it degrades (Jameela et al 1997). It has a regular structure and its melting temperature is above the body temperature. So, in the body, the semi-crystalline structure of PCL results in high toughness as the amorphous domains are in the rubbery state. It also has crystallisable rubbery properties due to which it has been widely utilized for improving elasticity. Its crystallinity tends to decrease with increasing molecular weight. The low melting point makes the material suited for composting as a means of disposal.

The main mode of degradation for caprolactone polymers is hydrolysis which proceeds by the diffusion of water into the material followed by random hydrolysis, fragmentation of the

material and a more extensive hydrolysis accompanied by phagocytosis, diffusion and metabolism. The hydrolysis is affected by the size, hydrophilicity and crystallinity of the polymer and pH and temperature of the environment (Lacoulonche et al 1999). The homopolymer PCL has a total degradation period of 2-4 years depending on the starting molecular weight of the device or implant (Holland and Tighe 1992). The erosion rate of nanofibrous matrices follows the order, PGA>PLGA>PLLA> PCL (You et al 2005). The degradation of PCL is very slow due to the presence of 5 hydrophobic -CH_2 moieties in its repeating units and its crystallinity is too strong to be hydrolysed. This makes PCL much more suitable for long-term degradation applications such as delivery of encapsulated molecules extending over 1 year. PCL degrades at a rate that is compatible with bone regeneration.

The superior rheological, mechanical and viscoelastic properties, non-immunogenicity, biostability, highly porous network for cellular support and dissolution in most of the organic solvents present PCL as a versatile biomaterial which has tremendous potential in TE and scaffold fabrication (Woodruff and Hutmacher 2010). Any polymer processing technology can be used to produce an enormous array of PCL scaffolds and its relatively inexpensive production routes compared to other aliphatic polyesters are hugely advantageous. The four major surface modification techniques namely, plasma treatment, coating, chemical treatment and blending are done to facilitate cell adhesion. They alter the chemical and physical properties of the surface by modifying the existing surface or by coating it with a different material. The optimal degree of surface hydrophilicity depends on the cell type and the specific method of surface modification. Functional groups can also be added to make the polymer more hydrophilic, adhesive or biocompatible so as to allow favourable cell responses. The ease of shaping and manufacture enables appropriate pore sizes to be conducive to tissue in-growth and controlled delivery of drugs. The modified PCL nanofibres can be used to fabricate a broad spectrum scaffolds for skin, cartilage, bone, heart etc. It is an ideal material which provides structural support during the repair of the nervous tissues and has also been used to effectively entrap antibiotic drugs. Hence, a PCL construct can be considered as a drug delivery system to enhance bone ingrowth and regeneration in the treatment of bone defects as it provides an environment that supports mineralized tissue formation.

Nevertheless, properties such as weak hydrophilicity, acidic nature of the degradation products, lack of bio-activity and neutral charge distribution have restricted its usage. The degradation of PCL systems having high molecular weights is remarkably slow and may require even 3 years for complete removal from the host body. The slow degradation profile makes PCL less attractive for TE applications. The prolonged degradation time should be decreased to adjust to the rate of new tissue formation. Preparation of PCL-based nanocomposites by loading inorganic reinforcing nanofillers such as graphene oxide, bioglass, calcium, forsterite and carbon nanotubes (CNTs) improves various properties of the PCL scaffolds.

1.1.2 Graphene Oxide as a Polymer Nanofiller

Graphene has become very popular in the field of materials science after Novoselov et al (2004) published their work about monocrystalline graphitic films for which they were awarded the Nobel Prize in the year 2010. This team found that graphene is a single atomic plane of an inert material (graphite) which can react reversibly with atomic hydrogen. It is a two dimensional layer of sp^2 hybridized carbon atoms that are packed densely in a hexagonal (honeycomb) lattice structure. They elaborated on the concept that graphene is a 'robust atomic-scale scaffold' which is very stable and has metallic properties and electrical conductivity. It is believed to be the mother of graphitic carbon materials like GO and CNTs and has drawn considerable interest as a multifunctional nanofiller.

Graphene oxide (GO) is a 2D layered nanomaterial prepared from natural graphite which can be easily exfoliated into monolayer sheets of thickness ± 0.2 nm. GO sheets have recently attracted substantial interest as a possible intermediate for the manufacture of graphene as they typically preserve the layer structure of the parent graphite. However, the layers are buckled and the interlayer spacing is about two times larger (~0.7 nm) than that of graphite. GO has strong covalent bonding within the layers and weak interlayer interaction due to the existence of hydrogen-bonding interactions between the intercalated water molecules. It is essentially a sheet that is only one atom thick consisting of large specific surface area, carboxylic groups at the edges and epoxy and hydroxyl groups on the basal planes. It possesses extraordinary

physicochemical, mechanical, electrical, optical, biological, thermal and magnetic properties. GO is intrinsically an insulator due to the disruption of its sp^2 bonding networks whose electrical conductivity can be improved by chemical and thermal treatments. It provides a suitable environment for tissue regeneration due to its superior biocompatibility and biomimetic properties when compared to the conventional inert biomaterials. The other advantages of GO include non-toxicity, low production cost, ease of chemical functionalization, lightweight, enhanced flexibility, hardness, stability, dispersibility and hydrophilicity (Shen et al 2012).

Synthesis of GO is relatively easier and scalable than that of graphene. Graphite is first oxidized using strong oxidants such as $KMnO_4$, $KClO_3$ and $NaNO_2$ in the presence of mineral acids like HNO_3 or H_2SO_4 to create graphite oxide (Hummers and Offeman 1958) which is a compound of carbon, oxygen and hydrogen in variable ratios. Oxygenated functionalities introduced into graphite expand the layer separation and makes the material hydrophilic which results in improved exfoliation and hydration in aqueous media. Further, exfoliation of the graphite oxide sheets to manufacture the nanoscale and monolayered GO sheets can be achieved through ultrasonication or magnetic stirring of colloidal suspension in water or organic solvents and rapid thermal heating in a furnace under inert atmosphere. GO is much lighter in colour than graphene due to the loss of electronic conjugation brought about by the oxidation. The linear increase in zeta potential which is a characteristic of the electrical properties of the interfacial layers and the successive increase in the oxidation quantity results in the formation of a greater number of electronegative functional groups in the oxidized GO. The aggressive oxidative processes induce the layers to lose their planarity and promote their separation. GO can be chemically or thermally restored to yield reduced graphene oxide (RGO) which is more difficult to disperse due to the absence of most of the oxygen groups and its tendency to create aggregates. RGO retains some of the defects of the GO and lacks the unique properties of the pristine, unfunctionalized graphene. The structures of graphene, GO and RGO are presented in Figure 3.

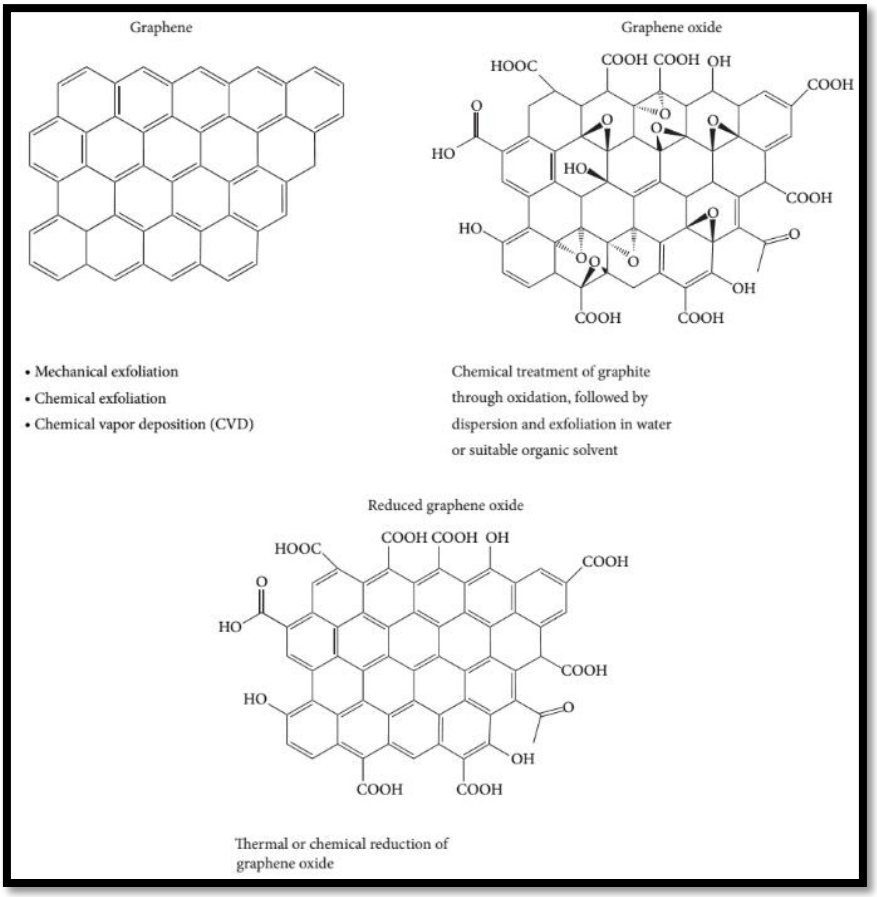

Figure 3 Structures of Graphene, GO and RGO (Dubey et al 2015)

Polar organic molecules and polymers including alcohols can easily be inserted into the GO lamellae to form intercalated composites which possess strong intermolecular forces such as hydrogen bonding and Coulomb forces (Liu et al 2000). Hence, GO offers plenty of opportunities for the cost-effective and large-scale preparation of composites with polymers, metals and ceramics which exhibit alterable multifunctional properties. The incorporation of GO into the polymers have shown large improvements in their structural, mechanical, thermal, electrical, biocompatible, topographical and barrier properties. It has created novel composites by expanding the functions and applications while retaining the excellent manufacturing and processing flexibility that is inherent to the polymers. The commonly used methods for the fabrication of polymer-based composite nanofibres are in-situ polymerization, solvent processing, casting, melt blending, electrospinning, self-assembly, phase separation and the use

of nanoporous templates. The high hydrophobicity of graphene undoubtedly limits its application in aqueous based preparation of composites. Furthermore, recent evidences indicate the unintended production of debris during the oxidation process. The most common technique used to overcome these problems is the chemical modification of the graphene sheets.

GO is more compatible with organic polymers than pristine graphene due to which homogeneous composites can be fabricated. It is amphiphilic as it has a large number of oxygenated functional groups such as epoxy (-C-O-C-), carbonyl (-C=O), carboxyl (-COOH) and hydroxyl (-OH) on its surface. They make the GO stable with uniform dispersions in some polar solvents due to the electrostatic repulsion and strong interactions with the polymer matrices and hence, facilitate the processing of GO-based composites by solvent blending. They increase the hydrophilicity, interfacial bonding strength, stress transfer, structural stability and bioactivity of the composites and lead to the formation of remarkable structural defects. The GO sheets can be easily functionalized with either the monomer or polymer chains due to the larger interlayer spacing and the presence of reactive functional groups. Thermal and solvent-based exfoliation techniques emerged as two preferred routes to increase the exfoliation degree of GO due to which the performance of the composites can be enhanced (Potts et al 2011). The presence of GO nanosheets substantially improves several properties such as robustness under bending, degradation rate and biological response of the PCL nanofibres in order to make them more usable in tissue engineering.

The unique structure-dependent properties have made GO greatly attractive for reinforcing the polymer composites that are used for various applications such as electronic circuits, shielding devices, structural and fuel efficient automotive components, memory and storage devices, sensors, coatings, flame retardants, packaging, catalysts and filtration as represented in Figure 4.

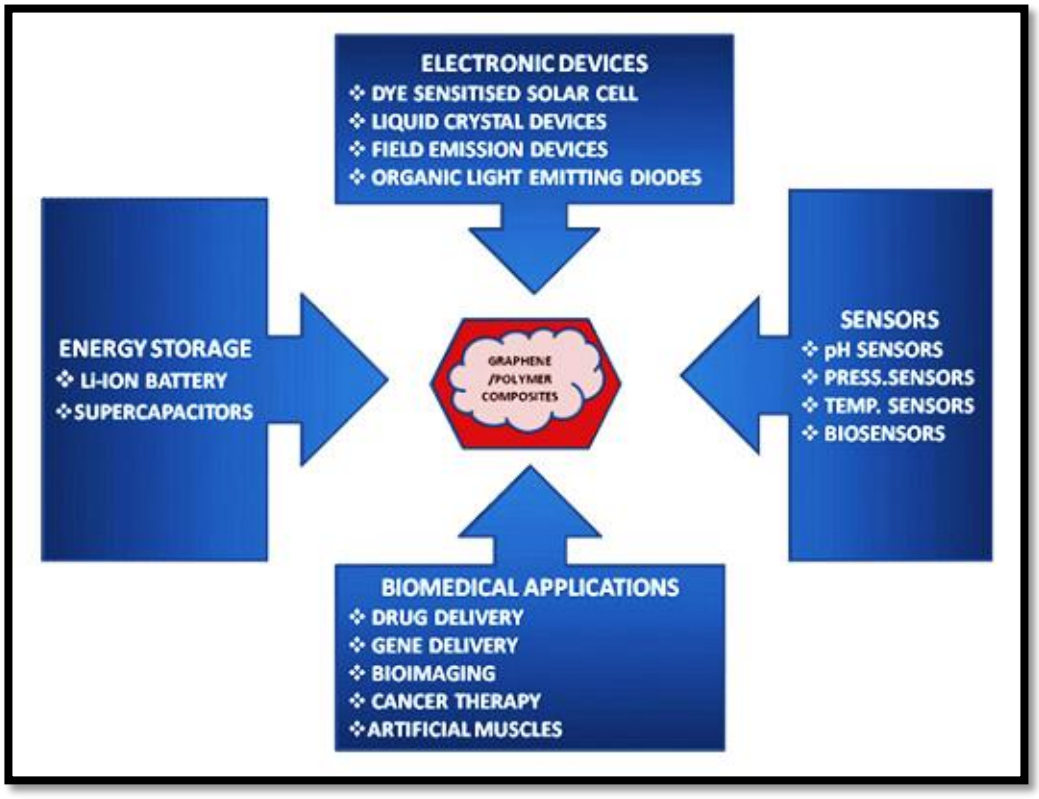

Figure 4 Applications of Graphene/Polymer Composites (Das and Prusty 2013)

The biomedical applications of GO-based composites which include proliferation and differentiation of stem cells, ultra miniaturized sensors, imaging, neural interfaces, delivery of drugs and genes, cell culture, photothermal cancer therapies, cellular probing and TE scaffolds are summarized in Figure 5. GO can efficiently bind the aromatic anticancer drugs, genes and proteins through π-π stacking, electrostatic and hydrophobic interactions.

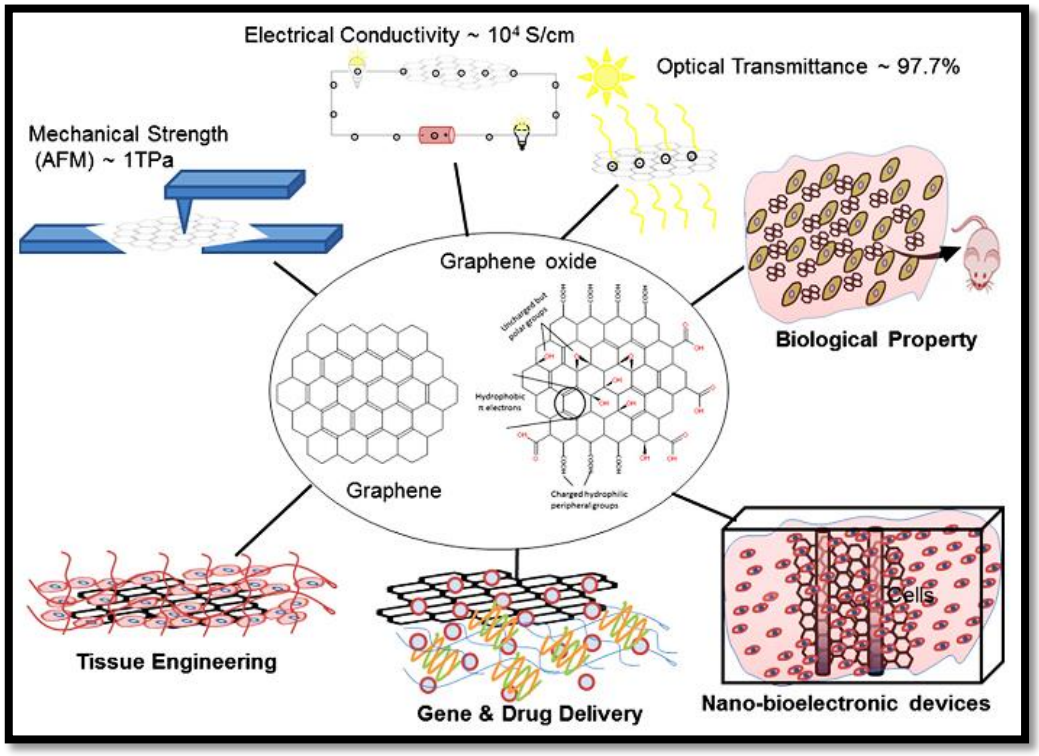

Figure 5 Biomedical Applications of GO-based Composites (Goenka et al 2014)

1.1.3 Fabrication Techniques

The major challenge of TE is the need for more complex functionality, biomechanical and functional stability in the laboratory-grown tissues destined for transplantation. Based on the structural pre-requisites, it is necessary to maintain high levels of accurate control over the macro (e.g., spatial form, mechanical strength, density, porosity) and microstructural (e.g., pore size, pore distribution, pore interconnectivity) properties during scaffold fabrication. A vast array of manufacturing techniques is available but, one must pay special attention to the scaffold specifications and also understand the interplay of factors affecting the material composition and design criteria. The key requirements necessary to assess a technique for scaffold production (Leong et al 2003) are:

- Processing conditions: Should not adversely affect the material properties, biocompatibility of the scaffolds and their subsequent clinical utility
- Process accuracy: Must be capable of producing spatially and anatomically accurate 3D scaffolds that fit the intended spaces at the implant site
- Consistency: Should produce scaffolds with highly consistent pore characteristics, size, morphology, distribution, density and interconnectivity in all the three dimensions
- Repeatability: Different scaffold batches should exhibit minimal variations in their physical forms and properties when produced from the same set of processing conditions and the technique must allow highly consistent and reproducible results to be achieved with ease
- Near-net shape fabrication and scalability for cost-effective industrial production

A variety of conventional manual-based production techniques are available which include fibre bonding, phase separation, solvent casting/particulate leaching, membrane lamination, melt moulding, gas foaming/high pressure processing, hydrocarbon templating, freeze drying and combinations of these processes. Most of these methods are tailored to create scaffolds that will meet the major requirements of only specific TE applications and are not usually generic. The main limitations are:

- Manual intervention: They are labour intensive, time-consuming, require multi-stage processing of the materials in order to form the desired scaffolds with the appropriate characteristics and heavily rely on the user skills and experiences which often result in inconsistent outcomes and poor repeatability
- Inconsistent and inflexible processing procedures: These techniques result in highly inconsistent macro and microstructural properties that are adverse to tissue regeneration
- Use of toxic organic solvents: They involve the extensive use of toxic organic solvents in order to convert the raw stock (granules, pellets or powders) into desired scaffolds and the incomplete removal especially in the thicker constructs will result in harmful residues that affect the adherent cells, incorporated biological active agents or nearby tissues

- Use of porogens: Salts or waxes employed as porogens limit the scaffolds to thin membranes (thickness = 2 mm) to facilitate complete porogen removal. Porogen particles entrapped by the matrix will agglomerate within the scaffold and require longer periods of soaking in water to leach the entire population due to which a high percentage of the drug payload can be lost. These factors will also result in uneven pore densities and morphologies that severely affect the material characteristics of the scaffold
- Shape limitations: The melt moulding technique is limited by the complexity in the design and construction of the mould. Membrane lamination method results in irregularly shaped scaffolds with limited interconnected pore networks

1.2 ELECTROSPINNING TECHNIQUE

The combined use of two processes namely, electrospraying and spinning is made use in a highly versatile technique called electrospinning (He et al 2011). It uses an electrical charge to draw very fine fibres (typically on the micro or nano scale) from a liquid. Electrospinning is a long-existing polymer processing method which was rediscovered in the early 1990s for its applications in the field of TE owing to its capability of generating nanofibrous constructs from a broad range of polymers in a simple setting and its feasibility for multiplexed functionalization. Both random and aligned nanofibrillar matrices can be fabricated from a variety of synthetic and natural polymers using electrospinning. This technique also offers the opportunity to control the thickness, composition and porosity of the nanofibres. It does not require the use of coagulation chemistry or high temperatures to produce solid threads from solutions which makes it particularly suited to the production of fibres from large and complex molecules. The polymer can be electrospun by either dissolving it in a suitable solvent or directly from a melt which ensures that no solvent can be carried over to the final product. Solution spinning results in a greater range of fibre sizes but, the melt spun fibres are typically limited to micron size or larger. The stable solutions can typically be electrospun at room temperature while the melts should be kept at elevated temperatures. Melt electrospinning eliminates the need for harsh organic solvents which is ideal for scaled-up processes and also the problem of inadequate solvent

evaporation between the capillary tip and the collector. However, the polymer must be able to cool sufficiently over this distance in order to generate fibres with a cylindrical morphology.

The other types of this technique are rotating roller electrospinning, wire electrospinning, bubble electrospinning, ball electrospinning, plate edge electrospinning, bowl electrospinning, hollow tube electrospinning, rotary cone electrospinning, spiral coil electrospinning, coaxial electrospinning and emulsion electrospinning. The wide range of applications of the electrospun fibres which has been presented in Figure 6 include filtering medium, membranes, catalysts, electronics, storage devices, non-woven, non-soiling and hydrophobic fabrics, insecticides, sensors, protective clothing for military, cosmetic creams and manufacture of nanocomposites. The electrospun fibres are also used for various applications in the medical field such as TE scaffolds, sutures, cardiac valve membranes, drug delivery systems, wound dressing materials, contraceptive devices, cancer diagnosis and therapy.

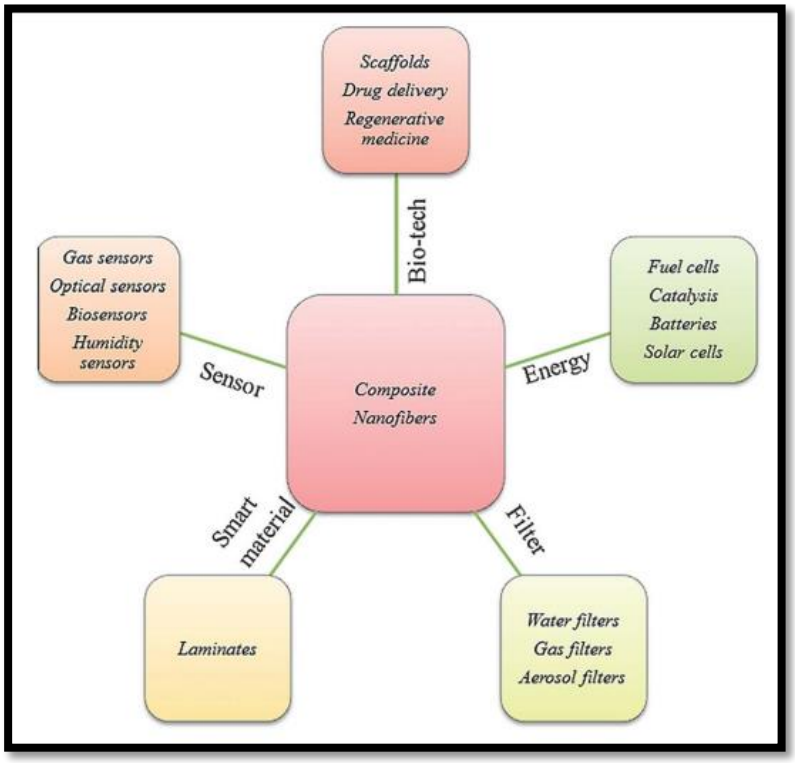

Figure 6 Applications of Electrospun Nanofibres (Sahay et al 2012)

The major components of a standard electrospinning setup (Figure 7) are:

- Spinneret (hypodermic syringe needle) connected to a high voltage (5 - 50 kV) direct current power supply
- Syringe pump
- Grounded collector

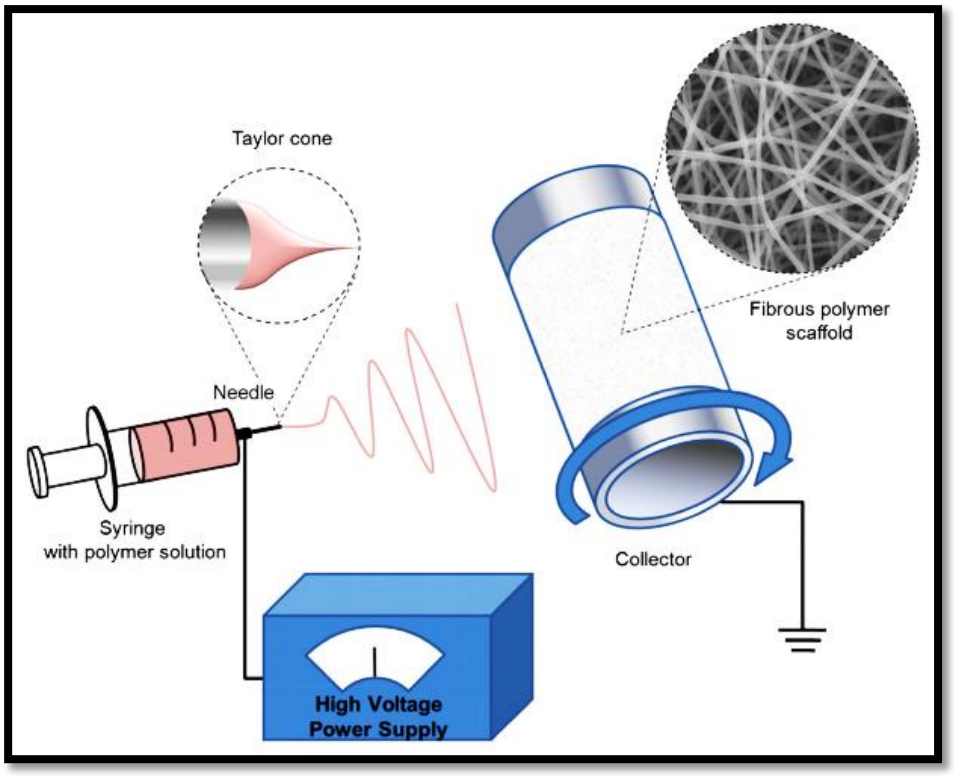

Figure 7 Electrospinning Setup (Rim et al 2013)

The polymer solution/sol-gel/particulate suspension/melt is loaded into the syringe (Merritt et al 2012) and a high voltage is applied on the liquid droplet. The body of the liquid becomes charged and the electrostatic force of repulsion counteracts the surface tension. The liquid is extruded from the needle tip at a constant rate by a syringe pump and the droplet eventually gets stretched. A stream of liquid erupts from the surface at a critical point and that point of eruption is called as Taylor cone. If the molecular cohesion of the liquid is sufficiently

high, stream breakup does not occur (if it does, the droplets are electrosprayed). A charged liquid jet is formed which gets dried in flight. The charge gets migrated to the surface of the fibre and the mode of current flow changes from ohmic to convective. The jet is elongated by a whipping process caused by the electrostatic repulsion initiated at the small bends in the fibre and finally gets deposited on the grounded collector. The elongation and thinning of the fibre is due to the bending instability. The droplet at the tip of the spinneret can be replenished by feeding from a header tank. A constant feed pressure is employed which is better for the lower viscosity feedstocks. Thus, continuous fibres are laid on the collector to form a non-woven fabric. The mechanism involved in the formation of fibres during the electrospinning process has been illustrated in Figure 8.

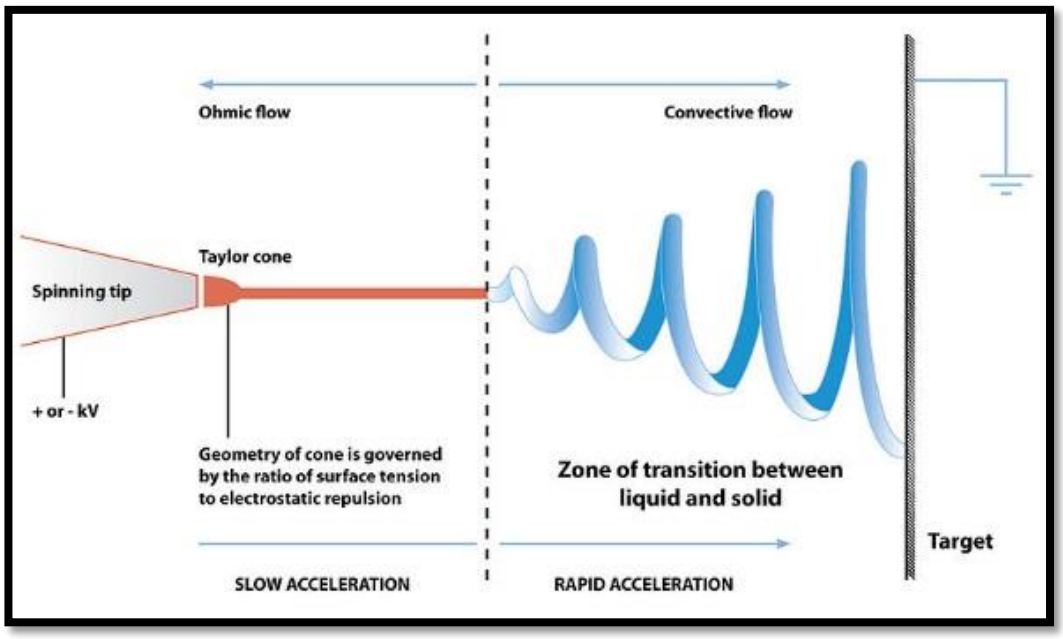

Figure 8 Mechanism of Fibre Formation (Kumar and Kumbhat 2016)

The various parameters that affect the electrospinning process include molecular weight and its distribution, architecture (branched, linear etc.), polydispersity index and T_g of the polymer; type, volatility and evaporation rate of the solvent; viscosity, concentration, conductivity, surface tension and flow rate of the solution; type, motion and size of collector;

temperature, humidity and air velocity of the chamber; configuration (single, side-by-side or coaxial) and diameter of the nozzle; distance between the tip and the collector, applied voltage, deposition time, gauge size of the needle, hydrostatic pressure in the capillary, electric potential at the tip, dielectric constant, type of additives used and configuration of the electrospinning setup (vertical or horizontal). The effect of some of the important parameters of electrospinning on the morphology of the resultant fibres is illustrated in Table 1.

Table 1 Effect of Electrospinning Parameters on Fibre Morphology (Sill and Recum 2008)

Parameter	Effect on fiber morphology
Applied voltage ↑	Fiber diameter ↓ initially, then ↑ (not monotonic)
Flow rate ↑	Fiber diameter ↑ (beaded morphologies occur if the flow rate is too high)
Distance between capillary and collector ↑	Fiber diameter ↓ (beaded morphologies occur if the distance between the capillary and collector is too short)
Polymer concentration (viscosity) ↑	Fiber diameter ↑ (within optimal range)
Solution conductivity ↑	Fiber diameter ↓ (broad diameter distribution)
Solvent volatility ↑	Fibers exhibit microtexture (pores on their surfaces, which increase surface area)

The numerous advantages of electrospinning over other processes are:

- Simple, straightforward, cheap, versatile, robust and dynamic process
- Mass production of nanofibres from various polymers
- Continuous ultrafine fibres having controlled structure, improved physical and chemical properties, high porosity, small pore size, large surface area to volume and length to diameter ratios

- Improved processability of fibres resulting in a variety of cross-sectional shapes and lengths (tunable morphology)

Electrospinning produces flexible, densely packed fibrous networks with tunable mechanical, physical, biological and tensile properties (McCullen et al 2012) based on the polymer selection, fibre size, network orientation and overall thickness. Electrospun nanofibres have been used as scaffolds for musculoskeletal (bone, cartilage, ligament and skeletal muscle), skin, vascular and neural TE applications and also as carriers for the controlled delivery of drugs, proteins and DNA. It is possible to generate loosely connected 3D porous scaffolds from natural and synthetic polymers. Aligned fibres having high porosity and fully interconnected pores can mimic the structure of ECM and aid in nutrient transport. The three-dimensional nature of the scaffolds allows the cells to infiltrate the matrix, proliferate and support the chondrocytes and stem cells. The capacity to adjust the fibre size is one of the greatest strengths of electrospinning. The non-woven mats comprised of nanofibres have a large fraction of surface which can be modified with a high density of bioactive molecules in order to make them ideal for cell attachment and interactions. They have the potential to overcome mass transfer limitations due to the high surface area to volume ratio and can afford greater drug loading. Nanofibrous electrospun scaffolds are considerably smaller than that of the microfibres produced using the conventional extrusion techniques. Hence, they are similar in size to the elements of the native ECM. Nanofibres affect the cellular behaviour by promoting the proliferation and differentiation of cells because of better attachment and organization around the fibres with diameters smaller than that of the cells. It is believed that the cell expression of phenotypic markers cannot be achieved if the scaffold fibre diameter is equivalent or larger than the cell. When formed as random mats, nanofibrous scaffolds exhibit isotropic mechanical properties reflective of their polymer composition. Due to the flexibility in material selection as well as the ability to control the properties, electrospun scaffolds have proved to be excellent candidates for various TE applications (Liu et al 2013).

1.3 OBJECTIVES

The major objectives of the present work are:

- To study the effect of various electrospinning parameters on the morphology of the PCL fibres
- To optimize the electrospinning conditions for the incorporation of GO into the PCL solutions
- To compare the PCL and PCL-GO electrospun fibres in terms of morphology, surface chemistry and mechanical behaviour

CHAPTER 2

REVIEW OF LITERATURE

2.1 PRODUCTION OF PCL-GO COMPOSITES THROUGH ELECTROSPINNING

The development of PCL-based composites reinforced with graphene, GO and RGO offers great potential in the field of tissue engineering. For successful production and improved performance, one of the key points is the full exfoliation and complete dispersion of the graphene nanofiller in the matrix. Due to the larger specific surface area, the exfoliated graphene sheets tend to form irreversible agglomerates or can even restack due to van der Waals interactions. Superior properties are tough to achieve due to the wrinkling and twisting of the sheets thereby, affecting the properties of the electrospun fibres. Moreover, the difficulty in controlling the curvature and alignment of the 2D graphene sheets in the limited nanoscale diameter may result in lowering the mechanical properties of the nanofibres. Proper incorporation of the GO sheets through electrospun nanofibres by simple blending with the polymer solution prior to electrospinning is a very difficult task because of the sheet dimensions. Hence, the formation of a polymer-GO covalent bond is more efficient than physical blending as it easily prevents the agglomeration and results in a uniform dispersion of GO (Wang et al 2011). If they are well dispersed in the polymer matrix, they form a highly oriented microstructure or co-continuous networks in the polymer. In order to produce homogeneous and smooth electrospun fibres, it is essential to prepare a good dispersion of the polymer and the fillers and also ensure that it remains stable in suspension during the electrospinning process. Several studies about the preparation and characterization of these types of fibrous systems are reported.

2.1.1 Mechanical Properties

Enhancement in the mechanical properties viz., tensile strength and Young’s modulus of the PCL/GO nanocomposites was observed by Ramazani and Karimi (2015). Wan and Chen

(2011) obtained higher energy at break of the PCL membrane when reinforced with GO nanoplatelets. The nanofibrous PCL/GO mats developed by Ramazani and Karimi (2016a) exhibited an increased shrink force and creep resistance. These improvements were mainly attributed to the strong interactions, intrinsic properties of GO and good dispersion of the nanosheets. The incorporation of GO, PCL-functionalized GO (fGO) and RGO increased the modulus and breaking stress of the PCL-based shape memory polyurethane (PU) nanofibres. The largest enhancement in the mechanical properties was observed in the fGO nanofibres due to the improved interaction between graphene and the polymer matrix. fGO and RGO-incorporated PU nanofibres showed faster actuation speed (Yoo et al 2014).

2.1.2 Biological Properties

Song et al (2015) suggested that the electrospun PCL/GO composite nanofibres could be a promising alternative material for biocompatible scaffolds for bone repair and regeneration, neural restoration and reconstruction due to the superior cell affinity, adhesion, spreading, growth and differentiation. The use of PCL/GO composite fibrous scaffolds as solid supports for the effective differentiation of the neural stem cells (NSCs) into oligodendrocytes was demonstrated by Uehara (2014) and Shah et al (2014). They also promoted the adhesion, proliferation and induced multi-nucleated myotube formation of human umbilical cord blood (UCB) derived mesenchymal stem cells (Chaudhuri et al 2014). The increased bioactivity of the PCL/GO composites stemmed from the anionic functional groups present on the GO surface that nucleate the formation of biominerals such as calcium phosphate (Wan and Chen 2011 and Ferrao 2015). The incorporation of thermally exfoliated graphene oxide (TEGO) into PCL-based scaffolds restricted the antimicrobial activity due to the presence of lower number of oxygen functional groups on the surface of TEGO than that of GO synthesized by Hummer's method (Okan et al 2016). A carbon nanomaterial mixture consisting of graphene nanoplatelets and single walled carbon nanotubes (SWCNTs) synthesized using plasma arc discharge method was incorporated into electrospun PCL microfibrous scaffolds with and without an additional poly-L-lysine surface coating. They hold great promise for improving the cartilage formation

due to enhanced cytocompatibility, growth of human bone marrow mesenchymal stem cells and chondrogenic differentiation (Holmes et al 2016).

2.1.3 Other Properties

The viscosity reduction of the PCL/GO solution was intensified by increasing the GO content and decreasing its oxidation level. The solution conductivity was enhanced by GO loading and the charge relaxation time grew due to higher content and oxidation level of GO (Ramazani and Karimi 2016b). The incorporation of GO into the PCL membrane increased the electrical conductivity and contact angle (Ferrao 2015).

2.2 FABRICATION OF PCL-GO COMPOSITES BY OTHER TECHNIQUES

2.2.1 Polymerization

GO was found to catalyze the ring opening polymerization of ε-caprolactone which enabled the conversion of the monomer into PCL. The carbon catalyst was retained and homogeneously dispersed within the polymer product resulting in the formation of a carbon-filled composite with improved mechanical stiffness. The carbon transitioned from the lamellar morphology that is primarily found in GO to nanometer sized, multi-walled fullerenes (Dreyer et al 2012). The PCL/graphite oxide composites synthesized by this method had decreased thermal stability and crystallization half-time. The increase in nucleation density clearly indicated that GO had an astounding nucleating effect on the crystallization of PCL due to good dispersion and better interaction (Hua et al 2007 a and b). Such composites were also fabricated in the presence of RGO and honeycomb-patterned thin films with regular structures were produced by casting the composite solution under humid conditions. Strong interaction, a good semiconducting behavior, increased thermal stability and DC conductivity were observed (Thinh et al 2012). If poly((R)-3-hydroxybutyric acid) (PHB) was used additionally, the biodegradability of the composite was accelerated (Thinh et al 2013). The PCL/GO nanocomposites manufactured by in situ polymerization exhibited homogeneous dispersion and

exfoliated structure of the GO nanosheets, high performances, novel functionalities, strong interfacial interaction, good solubility, excellent thermal stability and mechanical properties. The GO sheets bonded to the PCL chains acted as true nucleating agents to enhance the crystallization (Yu et al 2012, Wang et al 2012 and Wang et al 2013).

The PCL/Fe_3O_4/GO nanocomposites possessed increased crystallization temperature and decreased spherulite size as a result of heterogeneous nucleation effect and extraordinary paramagnetic behavior due to zero coercivity. Reduction of thermal stability of PCL was observed due to the fact that Fe_3O_4/GO acted as an effective catalyst for lowering the degradation temperature (Wang et al 2013). Yi et al (2015) developed in-situ polymerized hyperbranched polyurethane (HPU) composites with PCL-functionalized GO (f-GO) sheets. The wrinkled surface structure of GO was modified to a flat surface in f-GO owing to the PCL functionalization. The HPU/f-GO composites had significantly improved mechanical properties which was attributed to the presence of more interactive sites and better dispersion of the graphene sheets. They also demonstrated an excellent near-infrared laser-induced shape recovery and actuation speed as a result of the synergistic effect of PCL functionalization in the graphene and the hyperbranched structure of the matrix polymer.

2.2.2 Solution Mixing

Silylated graphite oxide (sGO)/PCL composites fabricated by solution blending method were found to have enhanced crystallization, mechanical properties and volume electrical conductivity due to higher interlayer space and dispersibility of the surface modified GO (Hua et al 2010). Biodegradable PCL/thermally reduced graphene (TRG) nanocomposites exhibited fine dispersion of TRG, strong interfacial adhesion, greater melt crystallization and storage modulus (Zhang and Qiu 2011). Wan and Chen (2012) prepared PCL/GO nanocomposites by solution mixing followed by drying and compression moulding which had a homogeneous dispersion of the nanoplatelets with high aspect ratios and improved stiffness, strength and ductility. The biodegradation of such composites was demonstrated by Balkova et al (2014) wherein GO served as nucleating agent and facilitated the absorption of cultivation media into

the composite thereby, increasing the decomposition onset temperature and matrix crystallinity degree. They concluded that GO was not a promoter of biodegradation.

2.2.3 Crystallization

Melt-crystallized films of PCL/GO were prepared by Kai et al (2008) through a conventional casting technique. They exhibited an enhanced Young's modulus, tensile strength and interlayer distance due to which more effective load transfer occurred. GO showed a nucleating effect towards the crystallization of PCL. Melt and solution crystallization of PCL on RGO resulted in improved interaction and mechanical properties (Wang et al 2013).

2.2.4 Melt Extrusion Printing & Covalent Linking

The graphene/PCL composites obtained by Cornock et al (2013) through coaxial melt extrusion printing have great potential as TE scaffolds, printed micro fluidic systems, biocompatible electronics, cell stimulators and advanced drug delivery platforms. This method was also used to prepare covalently linked graphene/PCL composites that possessed improved mechanical properties and biocompatibility (Sayyar et al 2014). Covalently linking PCL to the graphene chains through an esterification reaction resulted in enhanced homogeneity, processability, solubility, mechanical properties, electrical conductivity and biocompatibility (Sayyar et al 2013). The consistent, controllable and non-toxic degradation in conjunction with the notable physical and electronic properties confirmed that these composites are ideal materials for the development of TE scaffolds of electroresponsive cells (Murray et al 2015).

2.2.5 Solvent Precipitation

PCL/GO, PCL/RGO and PCL/amine-functionalized GO (AGO) composites were fabricated via solvent precipitation technique. The addition of the nanoparticles to PCL markedly increased the storage modulus which was largest for GO followed by AGO and RGO. The AGO and GO particles significantly improved the human mesenchymal stem cell

proliferation. AGO was most effective in augmenting stem cell osteogenesis leading to mineralization. The interaction with functionalized GO induced bacterial cell death because of membrane damage which was further accentuated by the amine groups in AGO. Hence, AGO composites were considered to be the best for inhibiting the biofilm formation due to the synergistic effect of oxygen containing functional groups and amine groups (Kumar et al 2015). Orthopedic implants (resorbable fracture fixation devices and tissue scaffolds) were designed by utilizing such PCL/GO and PCL/RGO nanocomposites. GO and RGO improved the mechanical properties of the PCL composites and influenced the surface water wettability. Pre-osteoblasts proliferated better on GO composites in 2D and on PCL in 3D. There was significantly higher differentiation and mineralization in 3D scaffolds due to the presence of organized multicellular aggregates (Kumar et al 2016).

2.2.6 Injection Moulding

Wang et al (2014) developed PCL/RGO nanocomposite bars having improved mechanical properties through injection moulding. It was demonstrated that RGO was an effective nucleation agent for PCL which enhanced the crystallization and orientation of the PCL chains in the flow direction by obstructing their motion.

2.2.7 Spin Coating

Poly(ethylenimine) (PEI) conjugated GO/PCL composite films were generated through spin coating. GO/PEI imparted strong multi-biofunctional properties to PCL as it significantly enhanced the antibacterial activity, surface wettability, surface roughness, modulus, proliferation and formation of focal adhesions in human mesenchymal stem cells (hMSCs) and was highly potent in inducing stem cell osteogenesis leading to near doubling of the alkaline phosphatase expression and mineralization. These nanocomposites can be used as an alternative to the labile biomolecules while preparing bioactive materials (Kumar et al 2016).

2.2.8 Solution Casting

Hassanzadeh et al (2016) produced 2D GO quantum dots (GOQDs) via microwave-assisted hydrothermal recycling of cellulose in waste paper and incorporated them as multifunctional property-enhancing additives for PCL by solution casting. The supramolecular assembly of the GOQDs controlled the morphology of the PCL films and also induced the mineralization on the surface. The concentration-dependent self-association of the GOQDs influenced the number of independent GOQD centers and tuned the number of nucleation points and subsequently, the size and density of the formed calcium phosphate crystals.

CHAPTER 3

MATERIALS AND METHODS

3.1 METHODOLOGY

The effect of several electrospinning parameters (polymer molecular weight, solvent system, concentration, flow rate, voltage and working distance) on the morphology of the electrospun fibres was investigated. After optimizing the electrospinning conditions, GO of various concentrations such as 0.1, 0.5 and 1 wt% was incorporated into the PCL solutions. The major aim was to study the effect of the nanosheets on the morphology, surface chemistry and mechanical behaviour of the fibres. Finally, a comparison between the PCL and PCL-GO electrospun fibres was drawn in order to establish new strategies for the fabrication of functionalized fibrous scaffolds for future TE applications. The methodology of the present study is briefly represented in Figure 9.

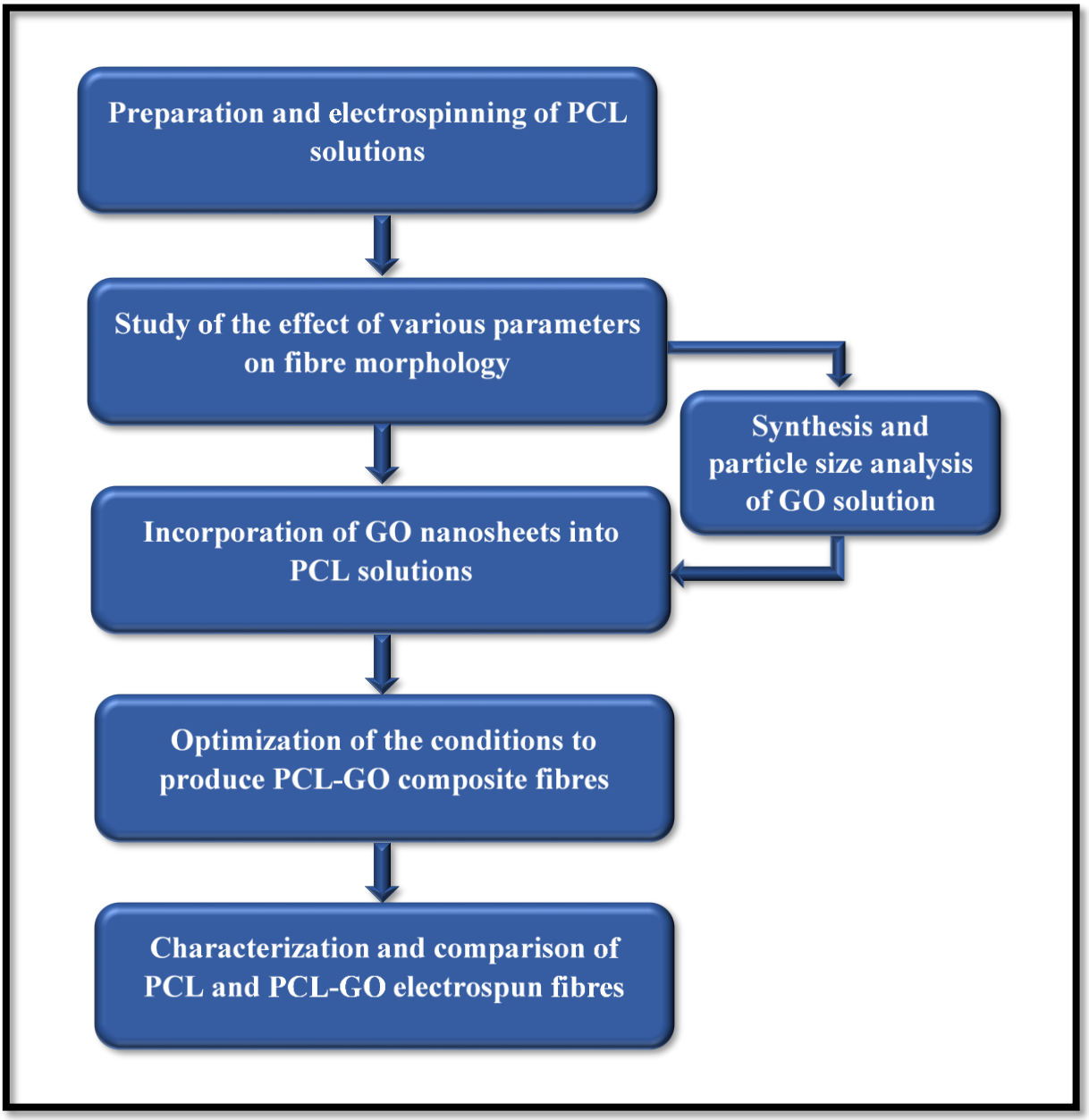

Figure 9 Methodology of the Study

Molecular weight of the polymer influences the solubility, crystallinity, polarity, cross-linking, rheological properties, electrical conductivity, dielectric strength, Trouton ratio ($\eta_{extensional}/\eta_{shear}$), surface tension wet spinnability, elongational flow, bending instability, jet branching, fibre initiation and stabilization. It plays an important role in determining the

minimum polymer concentration required to produce fine polymer fibres and in establishing the structure of the electrospun polymer. Hence, 2 different molecular weights of PCL, i.e, 45 and 80 kDa were employed in this study and their performance during electrospinning and effect on the fibre morphology were evaluated.

The polymer-solvent interactions determine the conformation of the polymer chain in a solution and the polymer solution properties are significantly affected by the solubility of the solvent. Manipulations of the solvent solubility influence the solution electrospinnability, viscoelasticity, critical minimum concentration of the solution in electrospinning. They also affect the diameter, crystallinity, tensile strength, aspect ratio and morphology of the electrospun polymeric fibres. PCL is readily soluble in a large range of organic common solvents and hydrolyses under physiological conditions into water-soluble monomers. A spinnability-solubility map of PCL was designed by Luo et al (2012) which is shown in Figure 10. Therefore, various solvents such as Chloroform, Methanol, Dimethylformamide (DMF), Dichloromethane (DCM) and their mixtures were utilized during this work.

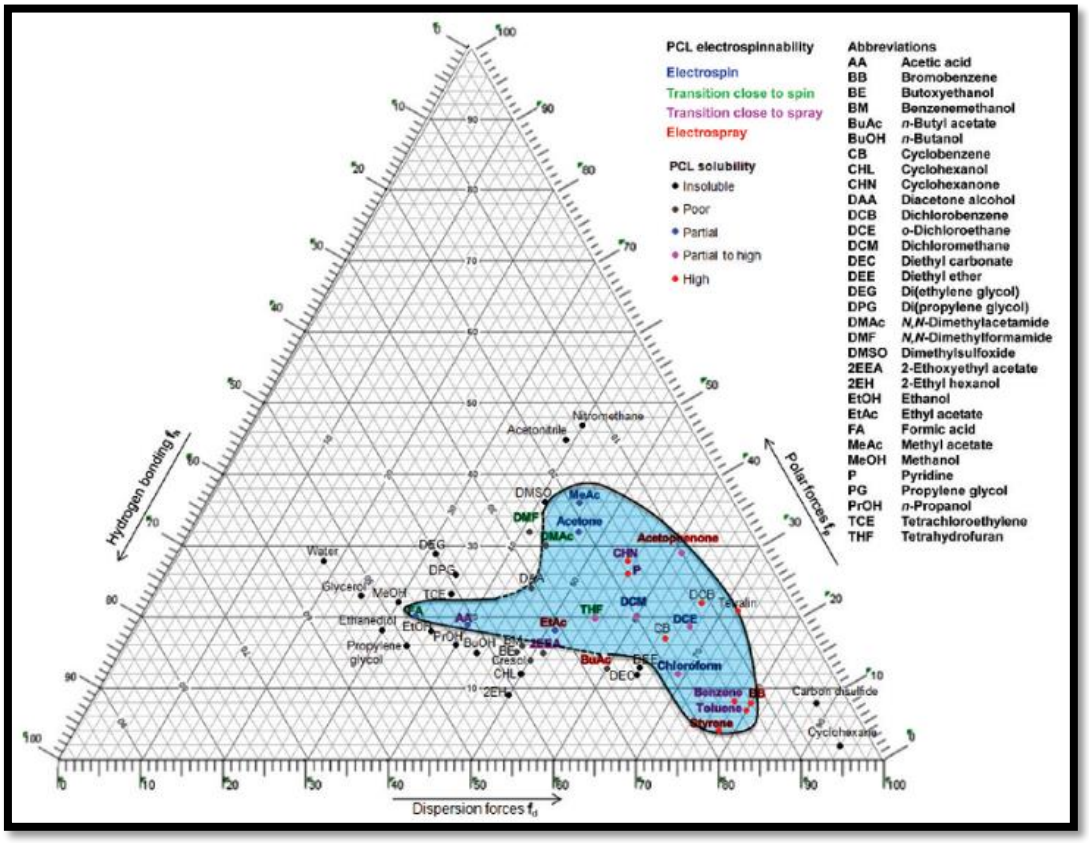

Figure 10 Spinnability-Solubility Map of PCL (Luo et al 2012)

3.2 CHEMICALS AND REAGENTS

The following chemicals and solvents were purchased from Sigma-Aldrich.

- PCL pellets having an average molecular weight of 45 kDa and 80 kDa
- Chloroform ($CHCl_3$)
- Methanol (CH_3OH)
- Dimethylformamide (DMF)
- Dichloromethane (DCM)

3.3 PREPARATION OF PCL AND GO SOLUTIONS

Different concentrations of PCL (M_n = 45 kDa and 80 kDa) were dissolved in the following solvent systems (Table 2):

Table 2 Preparation of PCL Solutions

Molecular Weight (kDa)	Concentration (w/v)	Solvent
45	8 and 12%	Chloroform
	7, 11, 12, 15 and 20%	Chloroform/Methanol 3:1 (v/v)
80	8, 10 and 15%	Chloroform/DMF 4:1 (v/v)
	12 and 15%	DCM/DMF 1:1 (v/v)
	12%	Chloroform/Methanol 1:1 and 3:1 (v/v)

An aqueous GO solution (4 mg/mL, water dispersion: Graphenea) was prepared and sonicated using a tip sonicator at intervals of 30 minutes for 3 hours. The major purpose of sonication was to reduce the original size of the GO sheets. After sonication, the GO solution was freeze-dried at -80°C by lyophilisation (Telstar LyoQuest HT-40, Beijer Electronics Products AB, Malmoe, Sweden). The GO sheets were then dispersed in DMF and in the solvent mixture of chloroform and methanol with 1:1 (v/v) ratio separately so as to obtain 2 solutions with a concentration of 3 mg/mL. The GO dispersions and PCL solutions were mixed to produce a series of PCL-GO compounds with GO concentrations of 0.1, 0.5 and 1 wt% which indicate the mass ratios of GO and PCL in the final mixture. All the electrospinning solutions were sealed tightly using a plastic film and stirred continuously at room temperature overnight by a magnetic stirrer to guarantee good dispersion.

3.4 ELECTROSPINNING

A conventional electrospinning procedure was adopted to fabricate pure PCL fibres and PCL-GO composites. The colloidal solutions were loaded into plastic syringes (HSW 6 mL) capped with stainless steel needles (Sterican Single-use Hypodermic Needles) having gauge sizes of 20G and 22G. They were then placed carefully in the Nanofibre Electrospinning Machine (NANON-01A, MECC Co. Ltd.) which is shown in Figure 11. The grounded plate collector was wrapped with aluminium foil in order to collect and observe the structure of the electrospun fibres. The electrical field was applied at various voltages of 13, 15, 18, 20, 25 and 30 kV by means of a high voltage power supply. Flow rates of 0.1, 0.2 and 1 mL/h and working distances (distance between the collector and the needle tip) of 12.5 and 15 cm were employed. A positively charged jet was formed from the Taylor cone and the fibres were deposited onto the target. Aligned fibre sheets which were required to carry out the mechanical tests were collected on a drum having a diameter of 200 mm and rotation speed of 1500 rpm. The experimental procedure has been summarized in Figure 12.

Figure 11 Nanofibre Electrospinning Machine

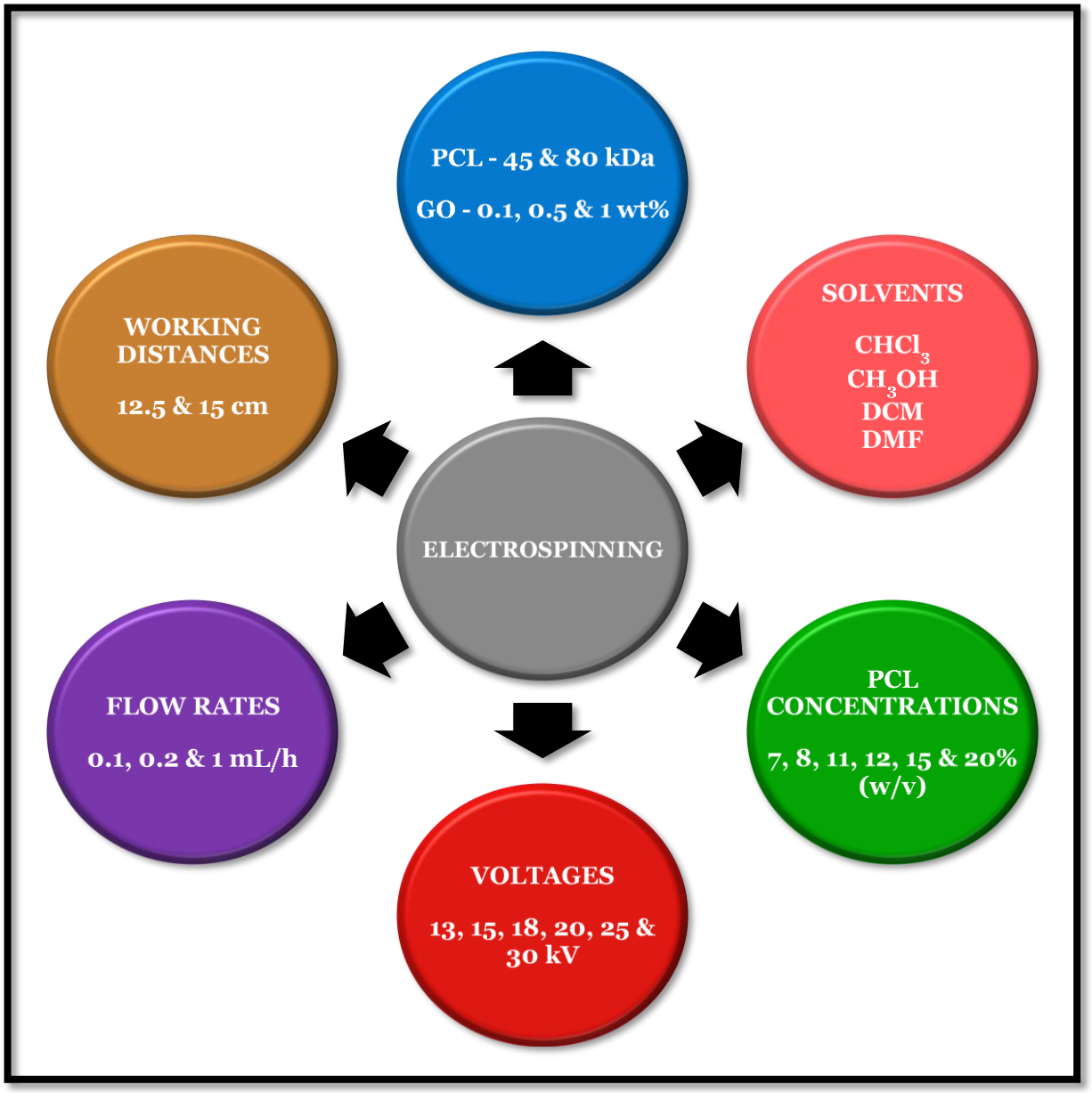

Figure 12 Fabrication of PCL and PCL-GO Composites by Electrospinning

3.5 STRUCTURAL AND CHEMICAL CHARACTERIZATION OF PCL FIBRES

The PCL pellets (M_n = 45 kDa) were dissolved in a solvent mixture of chloroform/methanol (3:1) and was poured onto a petri dish and allowed to dry overnight. This

was done to obtain a bulk PCL film which was employed as the standard during the XRD and FTIR analyses.

The XRD patterns of the electrospun mat and bulk film of PCL were observed using Shimadzu XRD-6100 Diffractometer. It is a high speed and high precision vertical goniometer with a compact design, safety interlocked system and independent dual axis θ-2θ linkage drive. The scans were carried out from 10° to 30° (2θ) at a rate of 2°/min using Ni-filtered CuK_{α} radiation.

FTIR data of both the samples were recorded using Perkin Elmer Spectrum1 FT-IR Spectrometer by dispersing the samples in KBr. The instrument has a scanning range of 450-4000 cm^{-1} and consists of globar and mercury vapour lamp as the sources, an interferometer chamber comprising of KBr and mylar beam splitters followed by a sample chamber and detector. Signal averaging, signal enhancement, base line correction and other spectral manipulations are also possible with this spectrometer which works under purged conditions and has a typical resolution of 1 cm^{-1}.

3.6 GO PARTICLE SIZE ANALYSIS

The size of the GO sheets was measured by the Dynamic Light Scattering (DLS) technique using a Zetasizer Nano ZS90 analyzer (Malvern Instruments, Malvern, UK). This equipment makes use of non-invasive back scatter (NIBS) technology to determine the particle size in the range of 0.6 nm to 6 mm.

3.7 OBSERVATION OF SURFACE MORPHOLOGY

The electrospun samples were sputter coated with a thin layer of gold to improve their electrical conductivity prior to SEM analysis. The surface morphology of all the samples were observed using Scanning Electron Microscope (Hitachi S-4100 SEM-EDS). The diameter of the fibres were calculated using Image J software from the SEM images.

3.8 ANALYSIS OF SURFACE CHEMISTRY

The functional groups present in pure PCL and PCL-GO composites were analyzed using Bruker RFS 100/S FT-Raman Spectrometer which has a resolution of 1 cm^{-1} and is equipped with the following components:

- Excitation source: Nd:YAG laser, 1064 nm, 500 mW, horizontally polarized (H)
- Michelson interferometer: Rocksolid configuration, permanently aligned
- Alignment excitation source: He-Ne laser, 633 nm, 1 mW
- Excitation radiation rejection: Notch filter
- Detector: Ge diode cooled at liquid nitrogen temperature of 77K

The distribution of the GO nanosheets inside the PCL fibres was observed using combined Raman-AFM-SNOM confocal microscope WITec alpha300 RAS+. A frequency doubled Nd:YAG laser operating at 532 nm was used as an excitation source with a power of 0.2 mW on the sample. Raman imaging experiments were performed by raster-scanning the laser beam over the samples and accumulating a full Raman spectrum at each pixel. The images were constructed by integrating specific bands using WITec software for data evaluation and processing.

3.9 MECHANICAL TESTS

The mechanical properties of the electrospun fibres were determined by a Micromaterial testing machine (Shimadzu MMT-101N) which utilized a stretching rate of 1 mm/min and gauge length of 25 mm. The PCL and PCL-GO fibrous mats were cut into rectangles having dimensions of 40 mm x 5mm x 0.15 mm (length x width x thickness). The elastic modulus of all the samples was calculated and compared.

CHAPTER 4

RESULTS AND DISCUSSION

4.1 CRYSTAL STRUCTURE OF PCL

PCL is a semi-crystalline polymer which has no diffraction peaks of other substances. Both the PCL samples contain three strong reflections at 2θ = 21.4°, 22° and 23.7° corresponding to the (110), (111) and (200) lattice planes of the orthorhombic crystal form respectively (Figure 13). The peaks are sharp and distinct which indicate that the sample is highly crystalline in nature. The PCL crystallites get uniformly oriented after the electrospinning process.

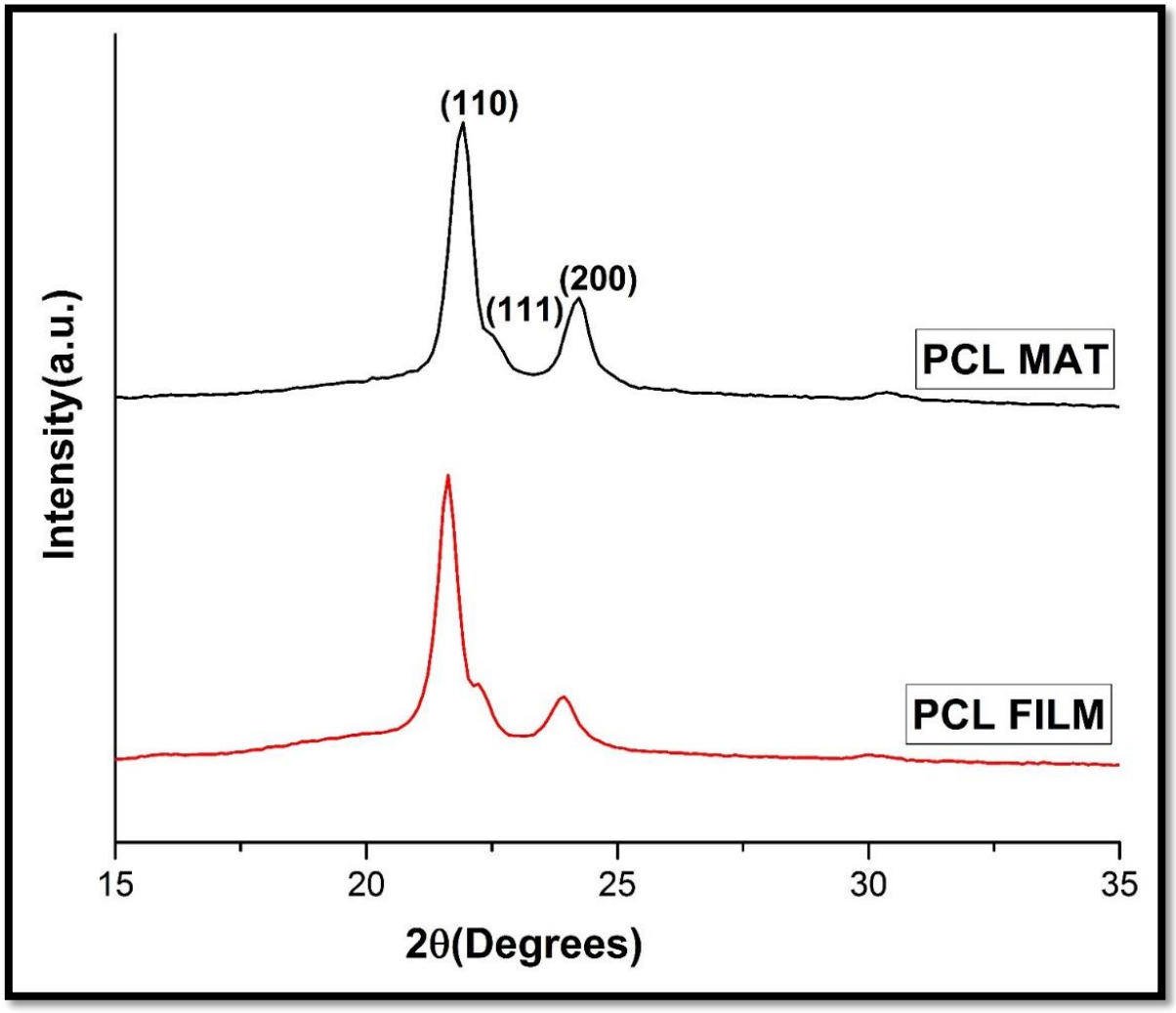

Figure 13 XRD Patterns of Electrospun Fibrous Mat and Bulk Film of PCL Dissolved in Chloroform/Methanol (3:1)

4.2 CHEMICAL ANALYSIS OF PCL

FTIR analysis was employed to identify any changes in the chemical structure that could have occurred during the electrospinning process. It was observed that electrospinning has no effect on the functional groups present in the resulting structure. No degradation had occurred and there were no residual solvents left at the end of this process. This is very beneficial for biomedical applications such as in scaffolds since the presence of solvent residues may harm

the growth of the cells and tissues. The characteristic peaks of the carbonyl groups (C=O) at 1720 cm^{-1} and aliphatic groups (C-H) at 2947 cm^{-1} (asymmetric CH_2 stretching) and 2865 cm^{-1} (symmetric CH_2 stretching) were observed in both the PCL samples. Other characteristic bands occurred at 1240 cm^{-1} (asymmetric C-O-C stretching) and 1170 cm^{-1} (symmetric C-O-C stretching) as shown in Figure 14. According to Coleman and Zarian (1979), the band at 1294 cm^{-1} is assigned to the backbone C-C and C-O stretching modes in the crystalline PCL. The peaks in the region of 1100-1190 cm^{-1} were observed only after the band de-convolution. He and Inoue (2000) established a procedure for the quantitative analysis of the crystallinity of PCL using a de-convolution of carbonyl vibration region (1726 cm^{-1}) into two bands namely, amorphous and crystalline. Due to the semi-crystalline nature of PCL, the absorption peak can be resolved by using a curve-fitting technique.

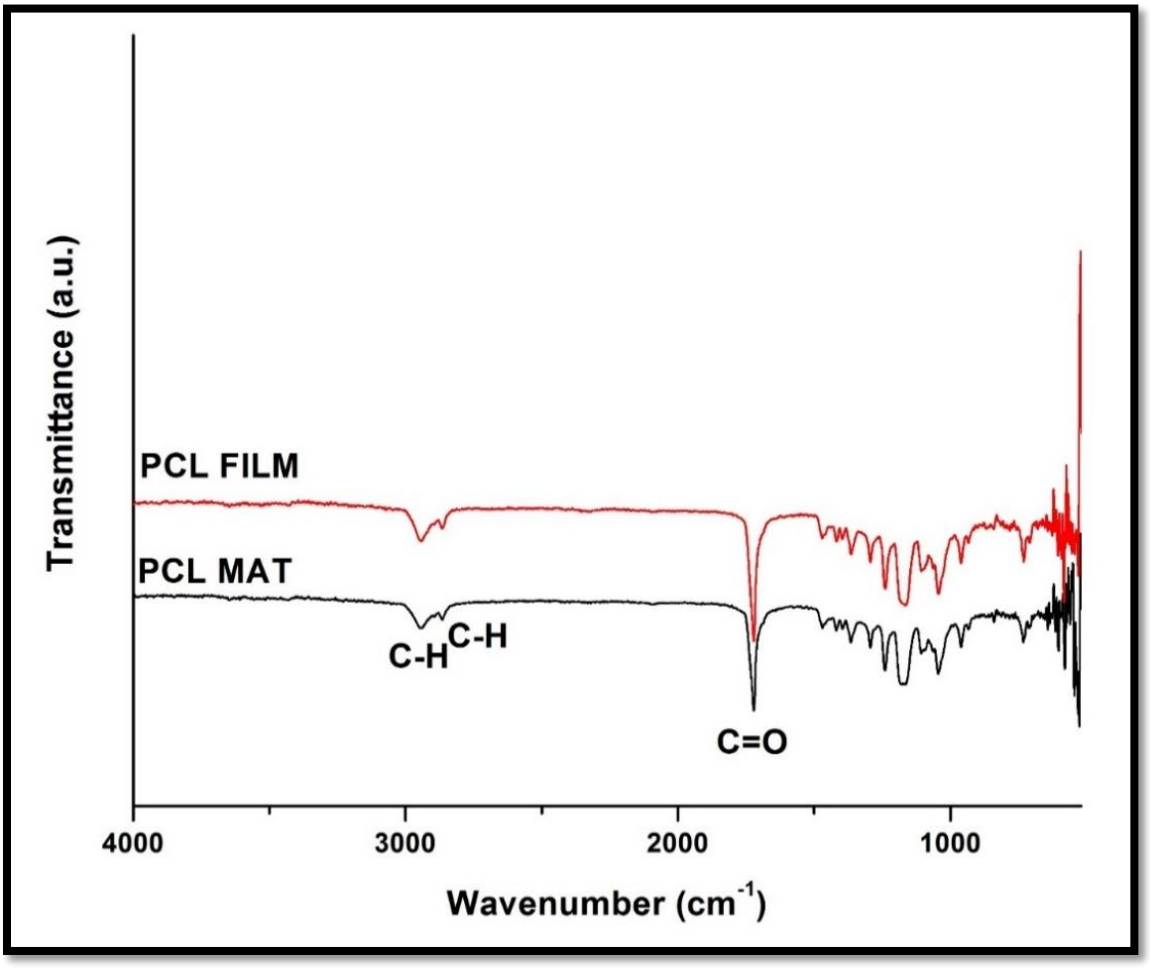

Figure 14 FTIR Spectra of Electrospun Fibrous Mat and Bulk Film of PCL Dissolved in Chloroform/Methanol (3:1)

4.3 PARTICLE SIZE DISTRIBUTION OF GO

The major reason for carrying out the sonication process was to reduce the GO sheets to an optimum size for proper incorporation into the fine PCL fibres without any damage or deterioration in the fibre properties. The size of the GO sheets underwent a sharp reduction during the first 2 hours of sonication (from 840 nm to 72 nm) after which it continued to decrease more gradually (from 72 nm to 45 nm). The sonication process broke down the van der Waals forces between the graphene layers and initiated the exfoliation process. The larger crystal size

of the parent graphite also favoured the exfoliation of GO and hence, yielded more quantities of monolayer sheets in shorter sonication times regardless of the C/O ratio. The presence of higher amount of hydroxyl groups that are preferentially located in the interior of the basal plane with a longer bonding distance than the epoxy groups created several areas of weakness which contributed to the breaking of the sheets. The reduction in the size of the GO sheets during the 3 hours of sonication has been illustrated in Table 3 and Figure 15.

Table 3 Observation of GO Size During Sonication

Diameter (nm)	Time (Hours)
840	0
316	1
72	2
45	3

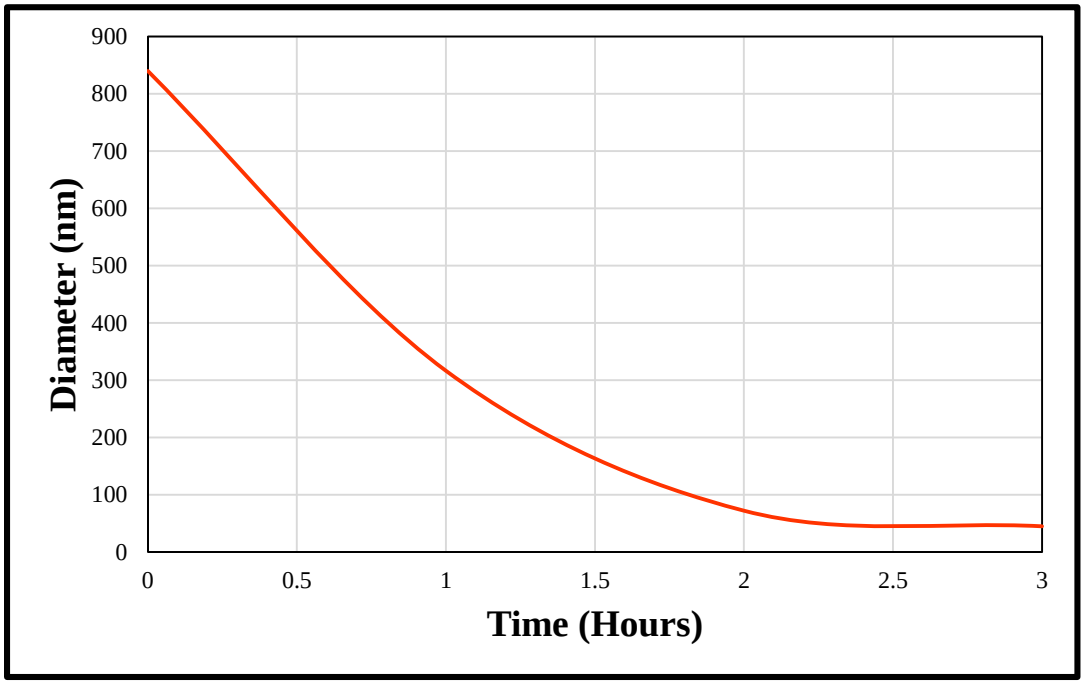

Figure 15 Size Reduction of GO Sheets

4.4 MORPHOLOGY OF THE FIBRES

4.4.1 Molecular Weight of 45 kDa

The major disadvantage of PCL scaffolds is their prolonged degradation period. A lower molecular weight (45 kDa) PCL sample is desirable to eliminate this problem as the biodegradation process is known to take place at a faster rate when the molecular weight of the polymer decreases. Electrospinning this sample using chloroform produced large spherical beads in the microstructure rather than a smooth fibrous network, irrespective of other conditions (Figure 16).

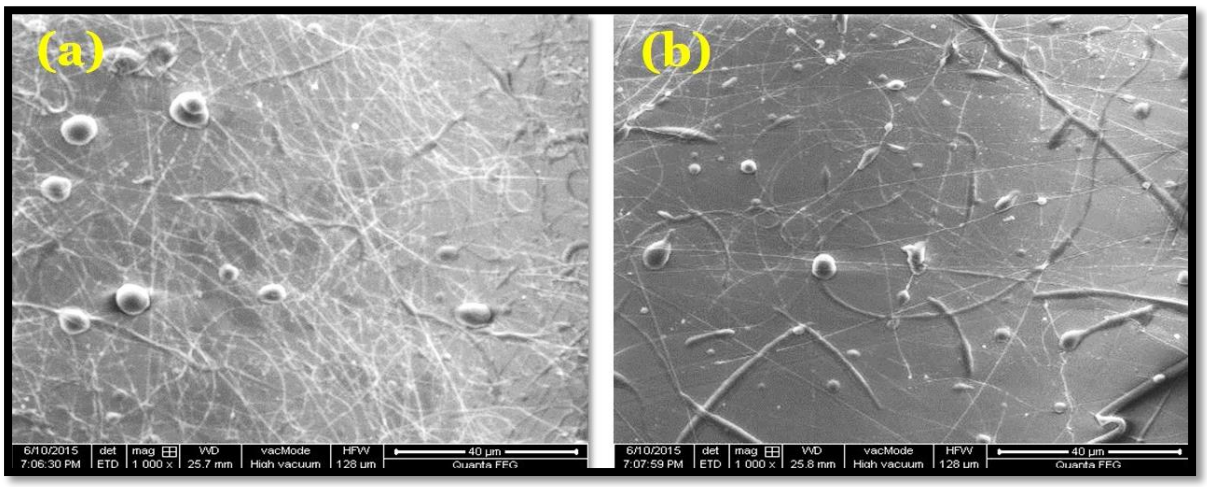

Figure 16 SEM Images of PCL Fibres Electrospun Using Chloroform at 0.1 mL/h and 15 cm
(a) 8%, 18 kV (b) 12%, 13 kV

The presence of beads was reduced significantly by the addition of a secondary solvent that improved the conductance of the polymeric solution. The addition of methanol, a poor solvent of PCL to pure chloroform resulted in bead-free fibres upto a concentration of 15%. The diameter of the fibres was found to increase with an increase in the voltage and decrease in the flow rate. PCL fibres electrospun from a solution of 12% concentration had the highest diameter.

On increasing the concentration to 15% and 20%, the diameter of the fibres decreased and resulted in the formation of beads. Hence, 12% was considered as the optimum concentration when a solvent system of chloroform and methanol (3:1) was used for electrospinning low molecular weight PCL samples (Figure 17).

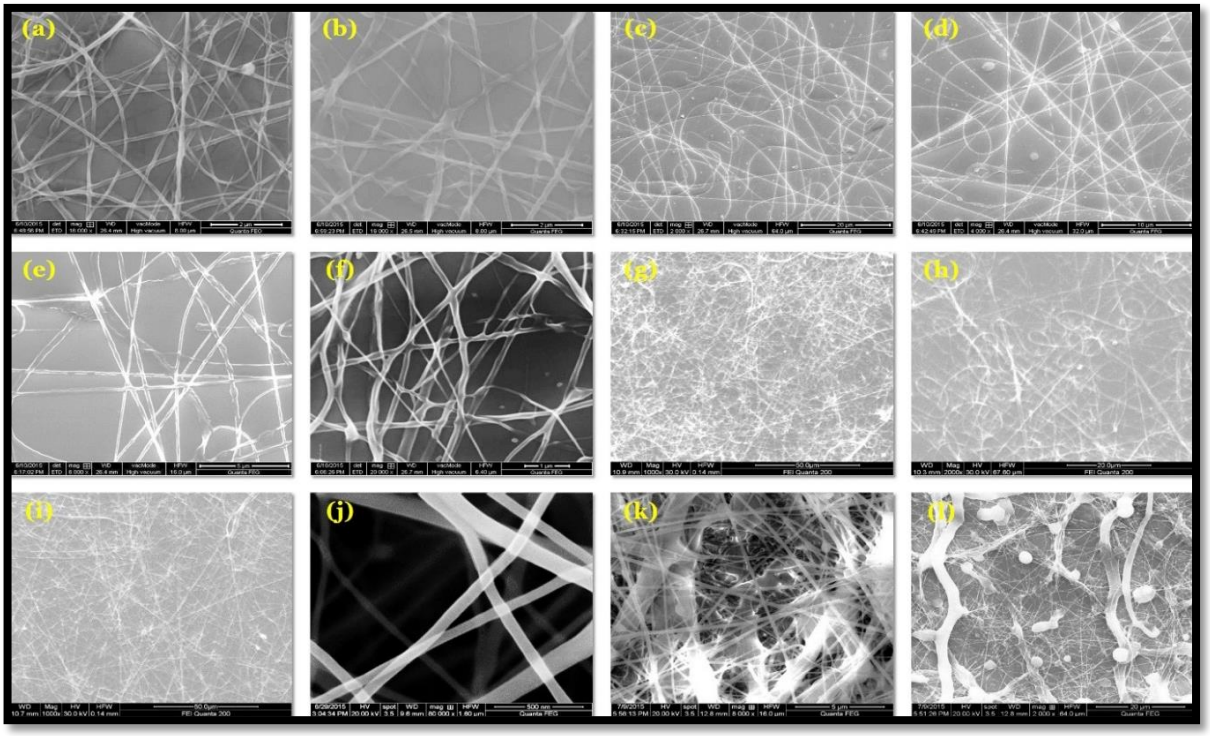

Figure 17 SEM Images of PCL Fibres Electrospun Using Chloroform/Methanol (3:1) at 15 cm

(a) 7%, 0.1 mL/h, 15 kV (b) 7%, 0.1 mL/h, 18 kV (c) 7 %, 0.2 mL/h, 15 kV
(d) 7%, 0.2 mL/h, 18 kV (e) 11%, 0.1 mL/h, 18 kV (f) 11%, 0.2 mL/h, 18 kV
(g) 12%, 0.1 mL/h, 15 kV (h) 12%, 0.1 mL/h, 18 kV (i) 12%, 0.2 mL/h, 15 kV
(j) 12%, 0.2 mL/h, 18 kV (k) 15%, 0.2 mL/h, 15 kV (l) 20%, 0.2 mL/h, 15 kV

The results interpreted from the above SEM images are summarized in Table 4.

Table 4 Morphology of Electrospun PCL Fibres (M_n = 45 kDa)

Solvent	Concentration (w/v)	Flow Rate (mL/h)	Voltage (kV)	Distance (cm)	Observations
Chloroform	8%	0.1	18	15	Large spherical beads
	12%	0.1	13	15	
Chloroform/Methanol 3:1 (v/v)	7%	0.1	15	15	Bead-free fibres
	7%	0.1	18	15	
	7%	0.2	15	15	
	7%	0.2	18	15	
	11%	0.1	18	15	
	11%	0.2	18	15	
	12%	0.1	15	15	
	12%	0.1	18	15	
	12%	0.2	15	15	
	12%	0.2	18	15	
	15%	0.2	15	15	
	20%	0.2	15	15	Presence of beads

4.4.2 Molecular Weight of 80 kDa

The main reason for utilizing high molecular weight PCL samples for the fabrication of scaffolds is the elimination of beads and droplets in the microstructure, despite its slow biodegradability. It is generally observed that on increasing the polymer molecular weight, the structure changes from beads to beaded fibres to complete fibres and finally to flat ribbons with greater fibre diameter. Spherical and spindle-shaped beaded fibres were produced during the

electrospinning of low concentrations (8 and 10%) of PCL solutions in chloroform/DMF (4:1) as illustrated in Figure 18. This was because electrospraying occurred instead of electrospinning owing to the low viscosity and high surface tension of the solutions and insufficient chain entanglements. A polymer solution must have a critical minimum concentration c_e to allow optimum molecular chain entanglements. Defect-free fibres can be obtained only when the solution concentration exceeds the critical concentration at which the physical interlocking of polymer chains occurs.

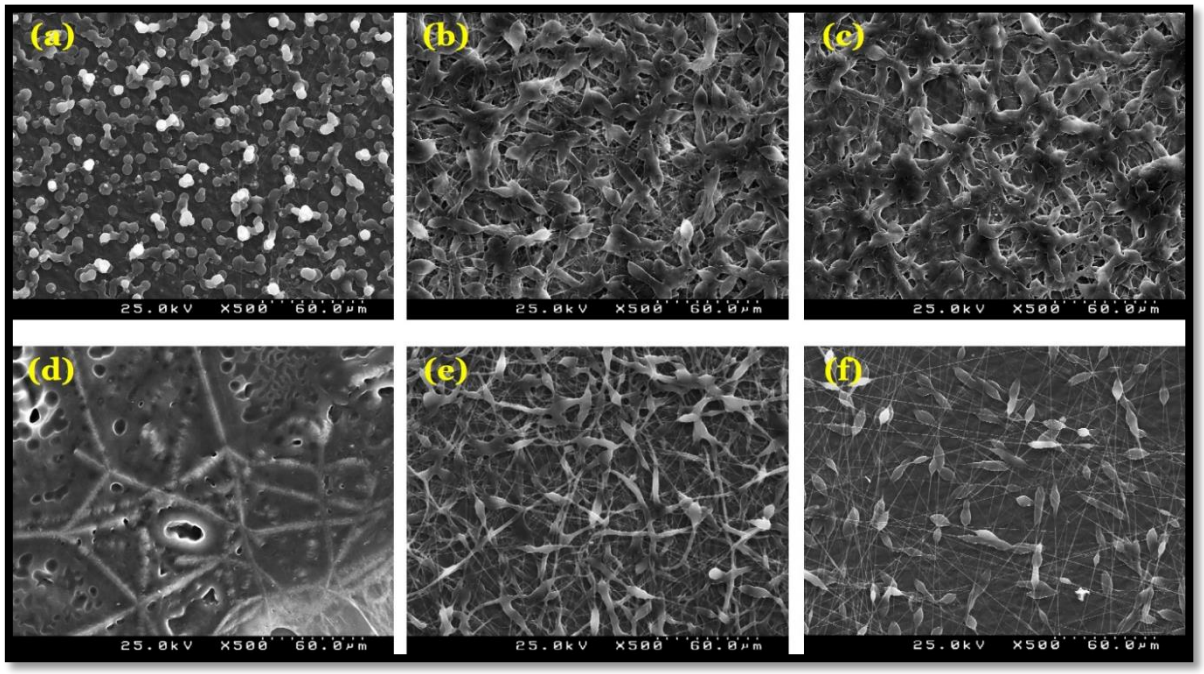

Figure 18 SEM Images of PCL Fibres Electrospun
Using Chloroform/DMF (4:1) at 1 mL/h

(a) 8%, 30 kV, 15 cm **(b) 10%, 25 kV, 12.5 cm** **(c) 10%, 30 kV, 12.5 cm**
(d) 10%, 20 kV, 15 cm **(e) 10%, 25 kV, 15 cm** **(f) 10%, 30 kV, 15 cm**

Increasing the solution concentration yielded bead-free and smooth fibres for both the solvent systems, chloroform/DMF (4:1) and DCM/DMF (1:1) as represented in Figure 19 and 20. Further, higher concentrations resulted in increased fibre diameter. DCM which is a commonly used solvent for PCL was not suitable for electrospinning because of its moderate

dielectric constant. The addition of DMF enhanced the spinning process and hence, uniform fibres were obtained due to higher viscosity. It was observed that only when the applied voltage was higher than the threshold voltage, the charged jet gets ejected from the Taylor cone. Uniformity and the diameter of the electrospun PCL fibres increased with increasing the voltage of the setup. It has been found that a minimum distance is required for the fibres to have sufficient time to dry before reaching the collector. At distances that are either too close or too far, beads were produced. Generally, lower flow rate is recommended as the polymer solution will have enough time for polarization. If the flow rate is very high, beaded fibres with thick diameter will form rather than smooth fibres with thin diameter owing to short drying time and low stretching forces.

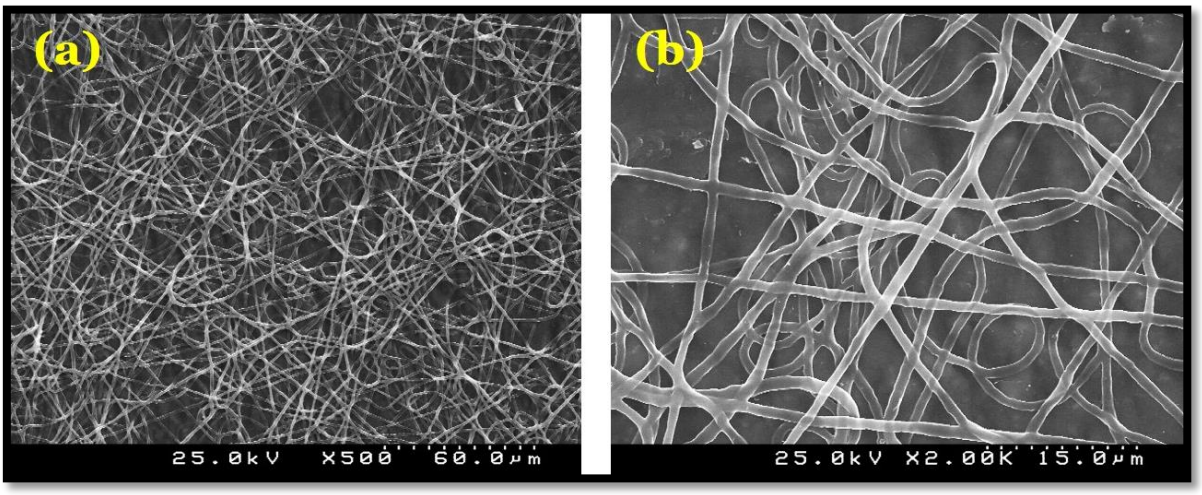

Figure 19 (a) and (b) SEM Images of 15% PCL Electrospun Fibres of Chloroform/DMF (4:1) System Under the Conditions of 0.2 mL/h, 30 kV, 15 cm

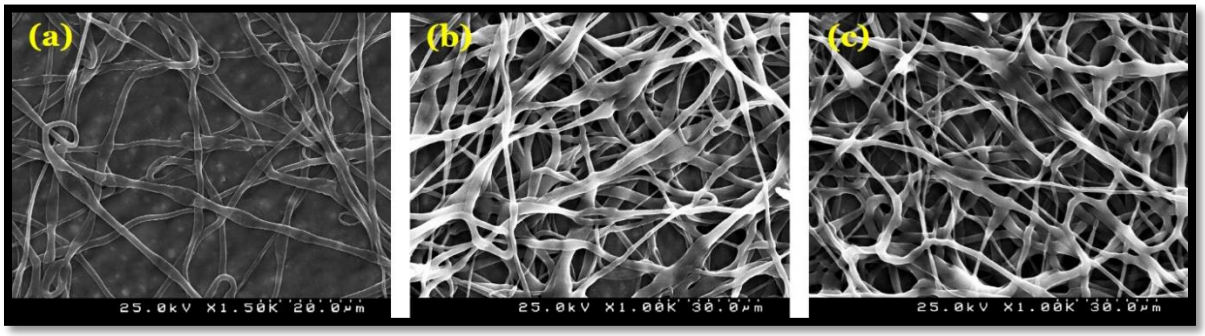

Figure 20 SEM Images of PCL Fibres Electrospun
Using DCM/DMF (1:1) at 1 mL/h and 15 cm
(a) 12%, 25 kV (b) 15%, 20 kV (c) 15%, 25 kV

PCL fibres of excellent quality and morphology and greater diameter were obtained when a solvent mixture of chloroform and methanol having 1:1 and 3:1 ratios was employed for electrospinning (Figure 21 and 22).

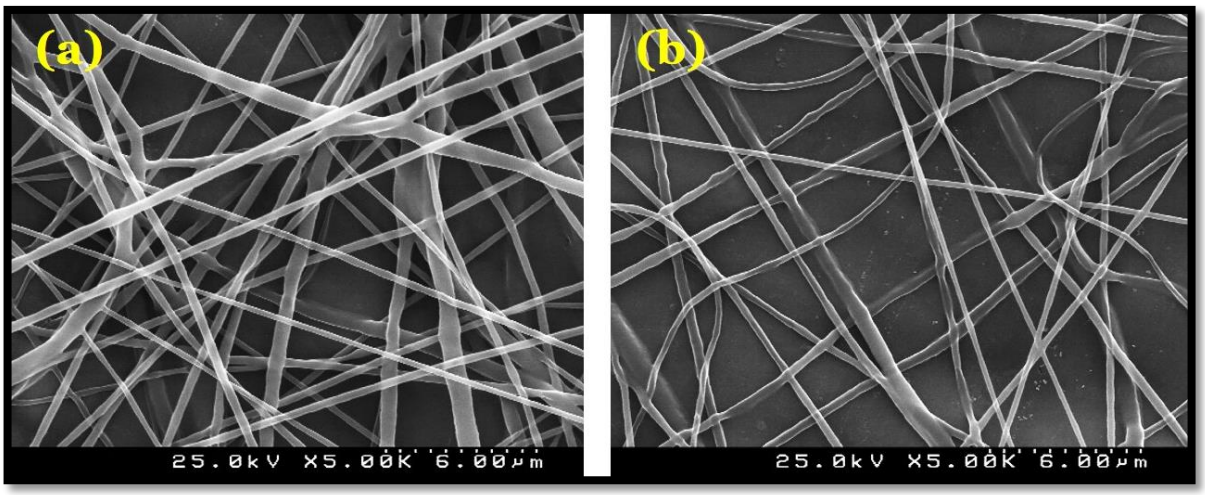

Figure 21 SEM Images of 12% PCL Fibres Electrospun Using
Chloroform/Methanol (1:1) at 1 mL/h and 15 cm
(a) 25 kV (b) 30 kV

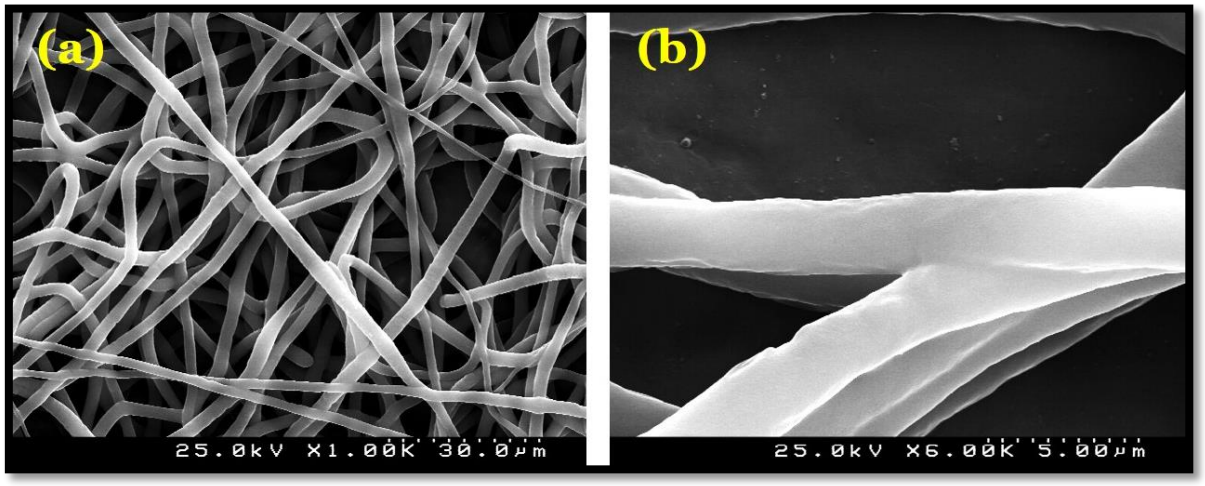

Figure 22 (a) and (b) SEM Images of 12% PCL Fibres Electrospun Using Chloroform/Methanol (3:1), 1 mL/h, 25 kV, 15 cm

During the electrospinning process, collectors usually act as the conductive substrate to collect the charged fibres. Aluminium foil is generally used as the collector but, it is difficult to transfer the deposited fibres to other substrates for various applications. In this study, fibres were also collected on a rotating cylindrical drum collector rather than a stationary target which has resulted in the formation of aligned fibres for mechanical tests.

The observations of the fibre morphology from the above SEM images are presented in Table 5.

Table 5 Morphology of PCL Fibres (M_n = 80 kDa)

Solvent	Concentration (w/v)	Flow Rate (mL/h)	Voltage (kV)	Distance (cm)	Observations
Chloroform/DMF 4:1 (v/v)	8%	1	30	15	Spherical and spindle-shaped beaded fibres
	10%	1	25	12.5	
	10%	1	30	12.5	
	10%	1	20	15	
	10%	1	25	15	
	10%	1	30	15	
	15%	0.2	30	15	Smooth and uniform fibres
DCM/DMF 1:1 (v/v)	12%	1	25	15	Bead-free fibres
	15%	1	20	15	
	15%	1	25	15	
Chloroform/Methanol 1:1 (v/v)	12%	1	25	15	Fibres of excellent quality
	12%	1	30	15	
Chloroform/Methanol 3:1 (v/v)	12%	1	25	15	

4.4.3 Effect of Incorporation of GO

The GO nanosheets were incorporated into the higher molecular weight (80 kDa) PCL solutions in order to obtain bead-free composite fibres. The 12%PCL-1%GO solution prepared using the solvent system of chloroform and methanol (1:1) was observed to have non-homogeneous distribution of the nanosheets as shown in Figure 23. The surface of the electrospun composite fibres was coarse due to the presence of grooves and protuberances (Figure 24).

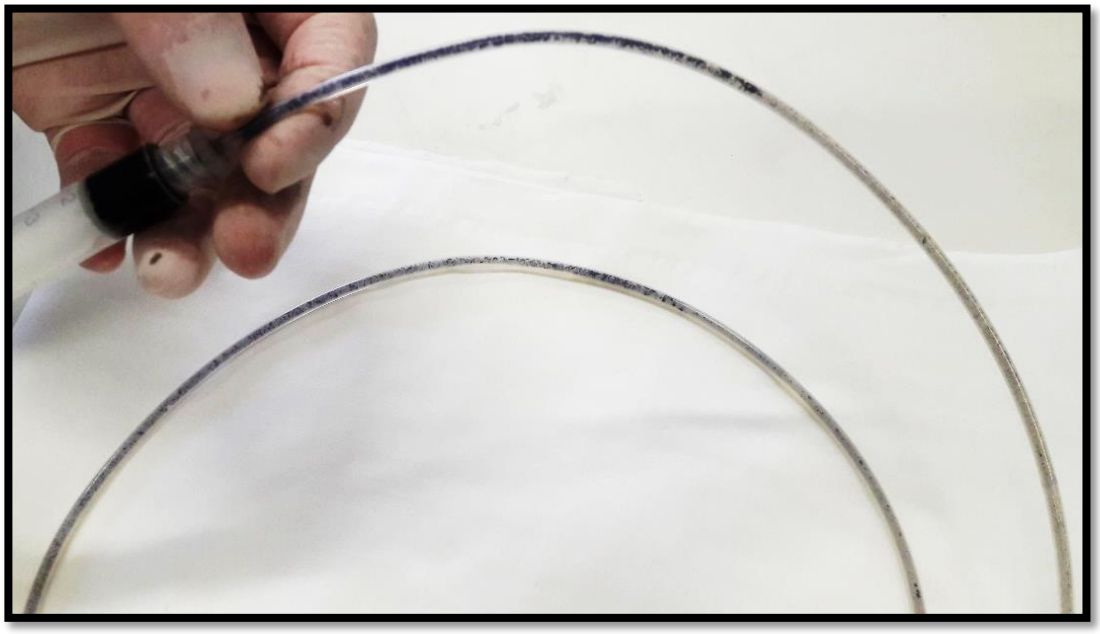

Figure 23 Non-Homogeneous Distribution of GO in PCL Before Electrospinning

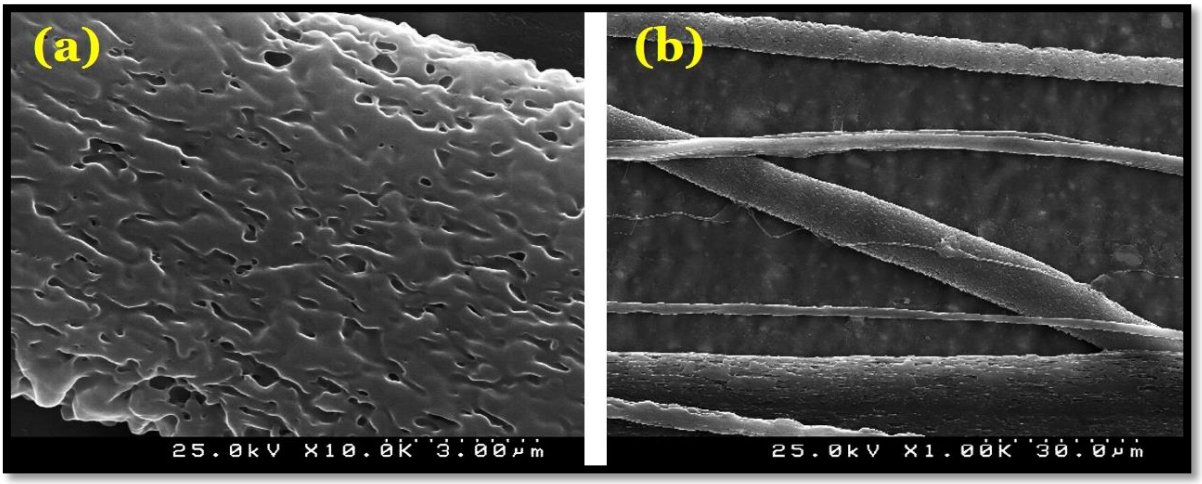

Figure 24 (a) and (b) SEM Images of 12%PCL-1%GO Composite Fibres Electrospun Using Chloroform/Methanol (1:1) System

When a 12% PCL-0.5% GO solution was prepared using the same solvent mixture, it could not be utilized for electrospinning due to the formation of various layers i.e, PCL dissolved in chloroform at the bottom and GO dissolved in methanol at the top (Figure 25).

Figure 25 Separation of Various Layers in PCL-GO Solution

Taking all these into consideration, the mixture of DCM and DMF (1:1) was chosen as the optimum solvent system for the incorporation of GO into PCL. It was observed that smooth fibres without any beads could be fabricated. The PCL-GO composite fibres were randomly oriented and possessed a three-dimensional interconnected porous structure which was similar to that of the pure PCL fibres. The SEM images show that the incorporation of GO can contribute to a more homogeneous distribution of the fibre dimensions and improved morphology as observed from Figure 26. The average diameter of these fibres decreased while the surface became rougher and more irregular with an increase in the GO loading. This may be attributed to dense stacking of the nanosheets whose size is larger than the diameter of the fibres and strong electrostatic interactions between the negatively charged GO sheets and the positively charged

PCL matrix. The fibre diameter gradually increased with increasing the applied voltage as the charged jet travelled faster to the collector and the solvent had less time to evaporate.

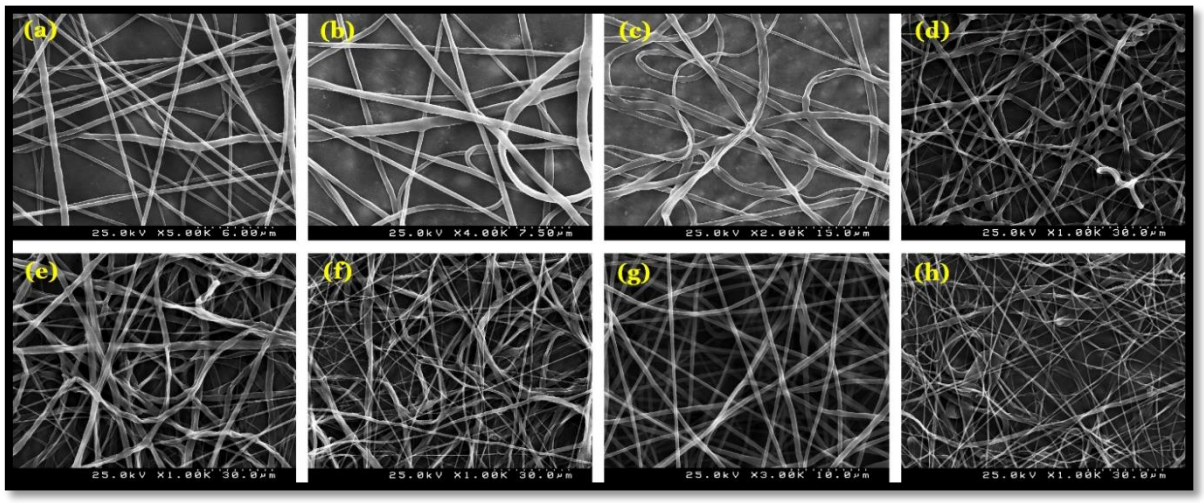

Figure 26 SEM Images of PCL-GO Composite Fibres Electrospun Using DCM/DMF (1:1) at 1 mL/h and 15 cm

(a) 12%PCL-0.1%GO, 20 kV **(b) 12%PCL-0.5%GO, 20 kV**

(c) 12%PCL-1%GO, 20 kV **(d) 15%PCL-0.1%GO, 20 kV**

(e) 15%PCL-0.1%GO, 25 kV **(f) 15%PCL-0.5%GO, 20 kV**

(g) 15%PCL-0.5%GO, 25 kV **(h) 15%PCL-1%GO, 20 kV**

The effect of introduction of the GO nanosheets on the morphology of PCL fibres is summarized in Table 6.

Table 6 Effect of Incorporation of GO Nanosheets on Fibre Morphology

Solvent	PCL Conc. (w/v)	GO Conc. (wt%)	Flow Rate (mL/h)	Voltage (kV)	Distance (cm)	Observations
Chloroform/Methanol 1:1 (v/v)	12%	0.5%	-	-	-	Could not be electrospun
	12%	1%	1	20	15	Rough surface of fibres
DCM/DMF 1:1 (v/v)	12%	0.1%	1	20	15	Smooth, bead-free fibres
	12%	0.5%	1	20	15	
	12%	1%	1	20	15	
	15%	0.1%	1	20	15	
	15%	0.1%	1	25	15	
	15%	0.5%	1	20	15	
	15%	0.5%	1	25	15	
	15%	1%	1	20	15	

4.5 SURFACE CHEMISTRY ANALYSIS

The conformational changes occurring in the 12% PCL fibres which were electrospun using DCM/DMF (1:1) at various concentrations of GO were estimated from the Raman spectra (Figure 27). The 3 characteristic peaks of GO were observed at 1323, 1583 and 2600 cm^{-1} corresponding to the bands of D, G and 2G respectively. 2D peak is a second-order overtone of the D peak which plays an important role in the characterization of GO. The spectrum of pure PCL fibres consisted of peaks at 2919 and 1724 cm^{-1} which were attributed to the stretching vibrations of C-H and C=O respectively. The peak at 1440 cm^{-1} was due to the bending vibrations of C-H. Moreover, the peaks at 1303, 1109 and 913 cm^{-1} corresponded to the out-of-plane wagging vibration of C-H, skeletal stretching vibrations and stretching vibrations of C-C (C-COO groups) respectively. In the composite fibres, the spectra presented the peaks of PCL

and the specific peaks of D and G bands which revealed the successful incorporation of the GO sheets and their strong interactions with the polymer matrix. As the concentration of GO increased, the intensity of the characteristic polymer bands in the PCL-GO composite decreased or even disappeared while the D and G bands of GO could be clearly observed in all the spectra.

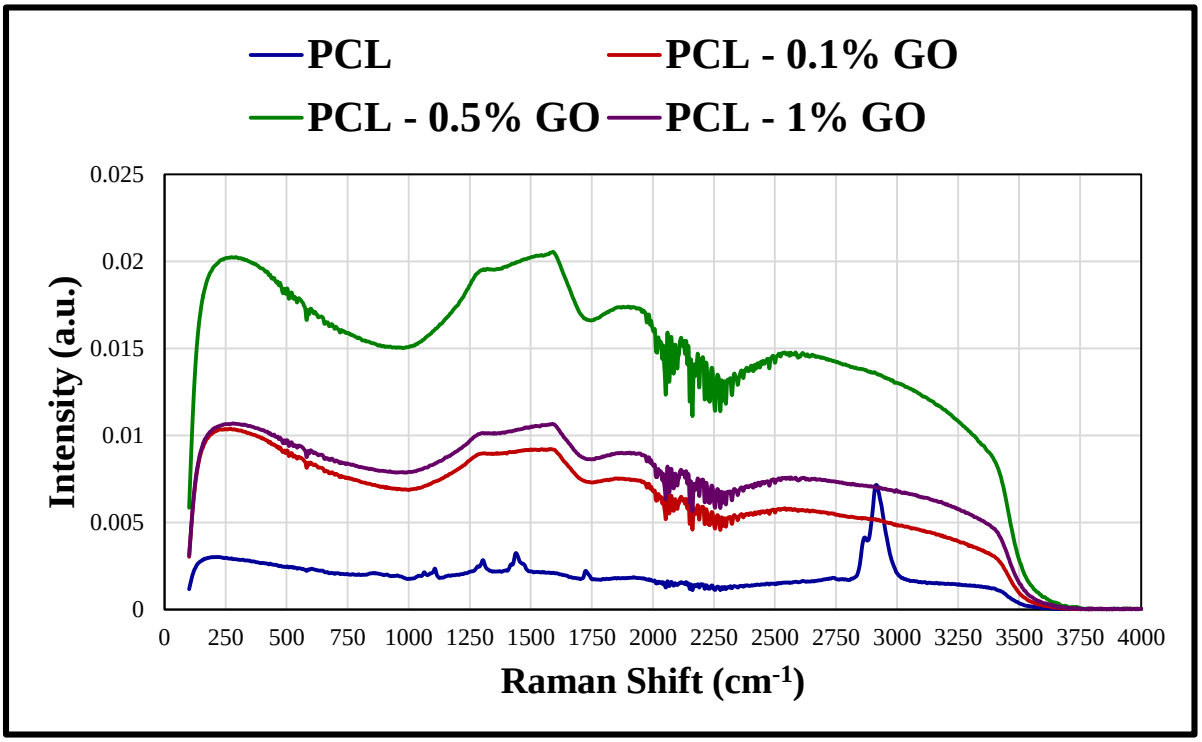

Figure 27 Raman Spectra of PCL and PCL-GO Composite Fibres

The Micro Raman spectra and images were obtained at different locations of the electrospun PCL-GO fibres in order to evaluate the distribution of the GO nanosheets inside them (Figure 28). In some areas, it was possible to detect only the presence of PCL while in other areas of the fibres, the GO nanosheets could be observed. The spectra consisted of the first order D band at 1350 cm^{-1} which was known to be the characteristic of structural disorder (oxidation) and G band at 1600 cm^{-1} that was associated with the structural graphitic order. The second order 2D band centred at 2615 cm^{-1} corresponding to the combination of the G and D modes represented the disturbed graphitic structure. In both cases, the most intense band of PCL at 2920 cm^{-1} was observed.

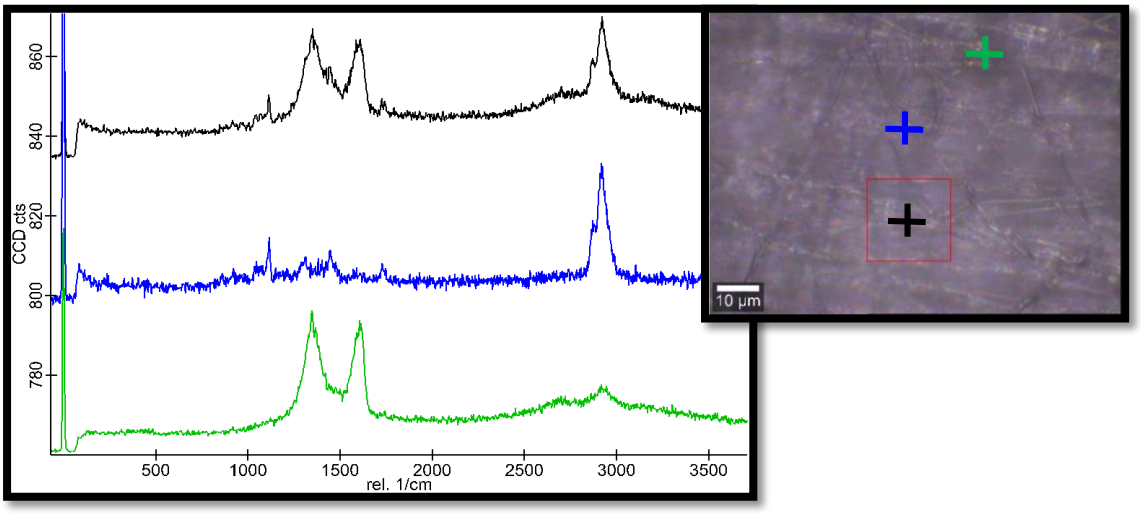

Figure 28 Raman Spectra and the Corresponding Confocal Images of the PCL-GO Fibrous Mats

From the confocal images of the combined Raman mapping of 1600 cm^{-1} (pink region) over 2920 cm^{-1} (blue region), the agglomeration of the GO nanosheets in the electrospun PCL fibres was evident (Figure 29).

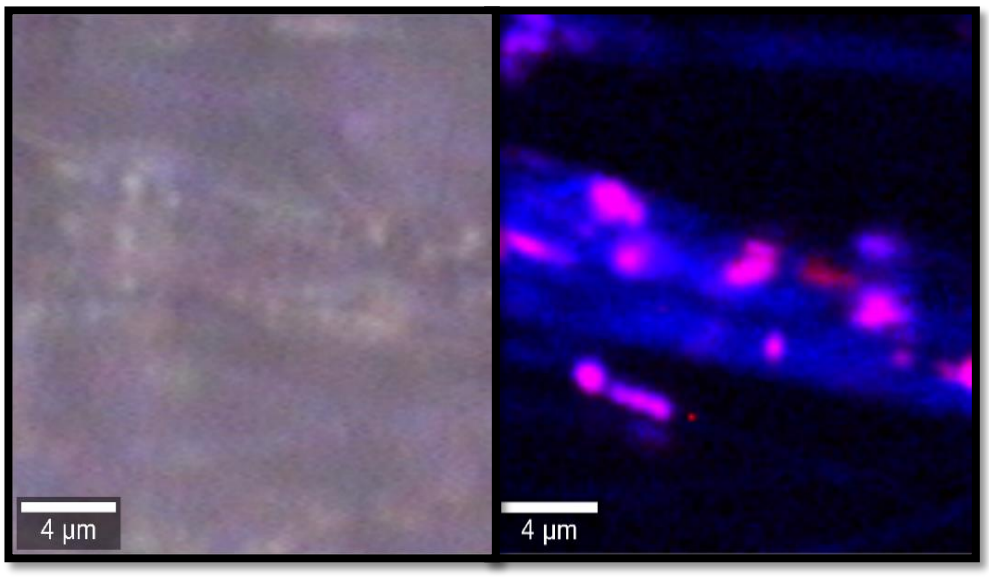

Figure 29 Combined Raman Mapping of 1600 cm^{-1} over 2920 cm^{-1}

The Raman spectra of the pink and blue regions of the fibres mainly represent the characteristic peaks of GO and PCL respectively (Figure 30).

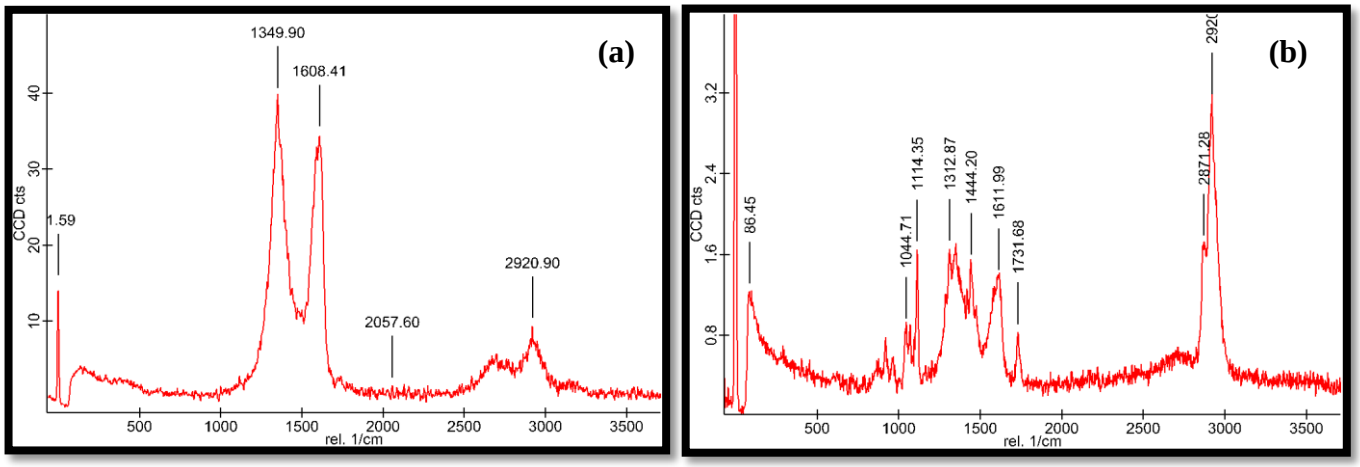

Figure 30 Raman Spectra Obtained by Combined Mapping of 1600 cm^{-1} over 2920 cm^{-1}
(a) Pink Region (b) Blue Region

4.6 MECHANICAL PROPERTIES

The mechanical properties of 12% PCL fibres electrospun using DCM/DMF (1:1) at various GO concentrations were evaluated using tensile testing as a function of the GO content. The PCL samples underwent a deformation that is characteristic of the semi-crystalline and ductile polymers exhibiting yielding, necking propagation and strain hardening. The stress-strain curves depicted that the overall deformation behaviour of the composite was also similar to that of PCL. The tensile stress and elastic modulus can be evaluated intuitively by the highest point of the ordinate and the line slope of the stress-strain curves respectively. The incorporation of GO remarkably increased the ultimate tensile strength and Young's modulus of the PCL fibres. The tensile strength of the PCL-GO composite fibrous mats having 0.1 wt% GO concentration was increased significantly which was attributed to the intrinsic properties of the GO nanosheets, homogeneous dispersion due to lower filler concentration and good adhesion in the PCL matrix. Moreover, the mechanical properties of the fibrous mats can also be related to the diameter and arrangement of the fibres. An increase in the fibre alignment and packing as

well as a decrease in the inter-fibre pore size and fibre diameter were found to enhance the mechanical properties of the electrospun mat. The highly wrinkled edges and flexible sheet-like structures of GO were able to crumple in the PCL matrix and hence, reduced the Poisson's ratio of the reinforced composite. They were capable of creating voids under stress by means of folding. The wrinkled morphology and abundant surface functionality of the GO sheets promise strong interfacial interactions with the PCL macromolecular chains which when coupled with higher aspect ratio, surface area, strength and stiffness result in superior mechanical properties of the composites.

However, when the concentration of GO was further increased, the tensile strength of the composites gradually decreased. When the concentration of GO was 0.5 wt%, the tensile strength of the composite became even lower than that of pure PCL. This was because the distance between the sheets became so small that they tend to stack together, making uniform dispersion and load transfer more difficult. The exfoliation of the nanosheets weakened due to the van der Waals force and consequently reduced the increment of the mechanical properties. The aggregated nanosheets disturb the matrix continuity and increase the stress concentration within the sample. Therefore, under the present experimental conditions, 0.1 wt% GO was considered to be the critical loading concentration for PCL. The elastic modulus of the PCL-GO composites also showed a similar trend with the increase of GO concentration i.e, it first increased and then decreased. Overall, the mechanical properties of the PCL-GO electrospun fibres were slightly exacerbated when the concentration of GO was increased to 0.5 wt%.

The values of the elastic modulus and the stress-strain curves of the PCL and PCL-GO electrospun fibres are presented in Table 7 and Figure 31 respectively.

Table 7 Elastic Modulus of PCL and PCL-GO Fibres

PCL Concentration (w/v)	GO Concentration (wt%)	Elastic Modulus (MPa)
12%	-	0.9017
12%	0.1%	1.0663
12%	0.5%	0.6082

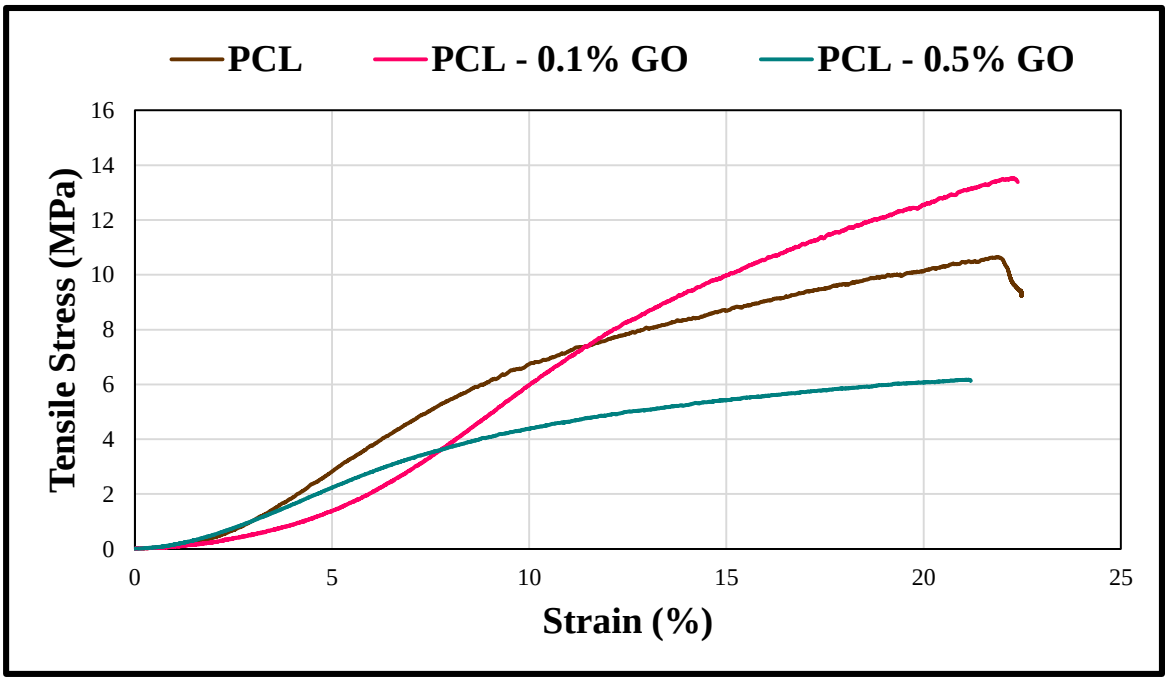

Figure 31 Stress-Strain Curves of PCL and PCL-GO Fibrous Mats

CHAPTER 5

SUMMARY AND CONCLUSIONS

The main aim of the present research was to fabricate biocompatible PCL and PCL-GO fibres for future tissue engineering applications through the electrospinning technology. The influence of various parameters viz., polymer molecular weight, solvent system, concentration, flow rate, voltage and working distance was studied by performing several characterization tests. The electrospinning conditions for the proper incorporation of GO into the PCL fibres were optimized. The effect of the nanosheets on the structure and properties of the electrospun fibres was investigated. It was found that the higher molecular weight (80 kDa) PCL samples were more suitable for the production of composite scaffolds due to the formation of defect-free fibres. The semi-crystalline nature of PCL was confirmed by the XRD analysis and the characteristic peaks of PCL was observed during FTIR spectroscopy. The GO sheets were subjected to sonication process to decrease their size so that they could be incorporated into the electrospun PCL fibres without any destruction. The solvent mixture of DCM/DMF (1:1) was considered to be the best solvent system for producing PCL-GO fibres. The addition of GO significantly improved the overall morphology of the PCL fibres and their average diameter decreased with the increasing concentration of the nanosheets. The Raman spectra revealed the presence of the characteristic peaks of both PCL and GO indicating strong interfacial interactions between them. The presence of lower concentrations of GO in the PCL fibres greatly enhanced the mechanical properties and 0.1 wt% GO was found to be the critical loading concentration for PCL. Hence, this study effectively demonstrated that the electrospun PCL composites embedded with the GO nanofillers are potential candidates for extensive applications in the field of tissue engineering.

REFERENCES

Balkova, R., Hermanova, S., Voberkova, S., Damborsky, P., Richtera, L., Omelkova, J. & Jancar, J., 2014, 'Structure and Morphology of Microbial Degraded Poly(ε-caprolactone)/Graphite Oxide Composite', Journal of Polymers and the Environment, 22, 2, 190-199.

Chaudhuri, B., Bhadra, D., Mondal, B. & Pramanik, K., 2014, 'Biocompatibility of electrospun graphene oxide-poly(ε-caprolactone) fibrous scaffolds with human cord blood mesenchymal stem cells derived skeletal myoblast', Materials Letters, 126, 109-112.

Coleman, M.M. & Zarian, J., 1979, 'Fourier transform infrared studies of polymer blends. II. Poly(ε-caprolactone)-poly(vinyl chloride) system', Journal of Polymer Science, 17, 5, 837-850.

Cornock, R., Beirne, S. & Wallace, G.G., 2013, 'Development of a Coaxial Melt Extrusion Printing Process for Specialised Composite Bioscaffold Fabrication', IEEE/ASME International Conference on Advanced Intelligent Mechatronics.

Das, T.K. & Prusty, S., 2013, 'Graphene-Based Polymer Composites and Their Applications', Polymer-Plastics Technology and Engineering, 52, 319-331.

Dreyer, D.R., Jarvis, K.A., Ferreira, P.J. & Bielawski, C.W., 2012, 'Graphite oxide as a carbocatalyst for the preparation of fullerene-reinforced polyester and polyamide nanocomposites', Polymer Chemistry, 3, 757.

Dubey, N., Bentini, R., Islam, I., Cao, T., Neto, A.H.C. & Rosa, V., 2015, 'Graphene: A Versatile Carbon-Based Material for Bone Tissue Engineering', Stem Cells International, 1-12.

Ferrão, M.P., 2015, 'Produção e Caracterização de Espumas 3D obtidas por Electrofiação para aplicação em Engenharia de Tecidos', Dissertação para obtenção do Grau de Mestre em Engenharia Biomédica, Faculdade de Ciências e Tecnologia, Universidade Nova de Lisboa.

Freed, L.E. & Guilak, F., 2007, Principles of Tissue Engineering, 3rd edition, 137.

Goenka, S., Sant, V. & Sant, S., 2014, 'Graphene-based nanomaterials for drug delivery and tissue engineering', Journal of Controlled Release, 173, 75-88.

Greenwald, A.S., Boden, S.D., Goldberg, V.M., Yaszemski, M. & Heim, C.S., 2006, 'Bone-Graft Substitutes: Facts, Fictions & Applications', American Academy of Orthopaedic Surgeons, 73rd Annual Meeting.

Hassanzadeh, S., Adolfsson, K.H., Wu, D. & Hakkarainen, M., 2016, 'Supramolecular Assembly of Biobased Graphene Oxide Quantum Dots Controls the Morphology of and Induces Mineralization on Poly(ε-caprolactone) Films', Biomacromolecules, 17, 256-261.

He, S.W., Li, S.S., Hu, Z.M., Yu, J.R., Chen, L. & Zhu, J., 2011, 'Effects of Three Parameters on the Diameter of Electrospun Poly(ethylene oxide) Nanofibers', Journal of Nanoscience and Nanotechnology, 11, 1052-1059.

He, Y. & Inoue, Y., 2000, 'Novel FTIR method for determining the crystallinity of poly(ε-caprolactone)', Polymer International, 49, 623-626.

Holland, S.J. & Tighe, B.J., 1992, 'Biodegradable Polymers', Advances in Pharmaceutical Science, 6, 101-164.

Holmes, B., Fang, X., Zarate, A., Keidar, M. & Zhang, L.G., 2016, 'Enhanced human bone marrow mesenchymal stem cell chondrogenic differentiation in electrospun constructs with carbon nanomaterials', Carbon, 97, 1-13.

Hua, L., Kai, W. & Inoue, Y., 2007a, 'Synthesis and characterization of poly(ε-caprolactone)-graphite oxide composites', Journal of Applied Polymer Science, 106, 1880-1884.

Hua, L., Kai, W. & Inoue, Y., 2007b, 'Crystallization behavior of poly(ε-caprolactone)/graphite oxide composites', Journal of Applied Polymer Science, 106, 4225-4232.

Hua, L., Kai, W., Liang, Z. & Inoue, Y., 2010, 'Polyester/organo-graphite oxide composite: Effect of organically surface modified layered graphite on structure and physical properties of poly(ε-caprolactone)', Journal of Polymer Science Part B: Polymer Physics, 48, 294-301.

Huang S.J., 1985, 'Biodegradable Polymers', Encyclopedia of Polymer Science and Engineering, 2, 220-243.

Hummers, W.S. & Offeman, R.E., 1958, 'Preparation of Graphitic Oxide', Journal of the American Chemical Society, 80, 6, 1339.

Jameela, S.R., Suma, N. & Jayakrishnan, A., 1997, 'Protein release from poly(ε-caprolactone) microspheres prepared by melt encapsulation and solvent evaporation techniques: A comparative study', Journal of Biomaterials Science, 8, 457-466.

Kai, W., Hirota, Y., Hua, L. & Inoue, Y., 2008, 'Thermal and mechanical properties of a poly(ε-caprolactone)/graphite oxide composite', Journal of Applied Polymer Science, 107, 1395-1400.

Kumar, N. & Kumbhat, S., 2016, 'Essentials in Nanoscience and Nanotechnology', 978-1-119-09611-5.

Kumar, S., Azam, M.D., Raj, S., Kolanthai, E., Vasu, K.S., Sood, A.K. & Chatterjee, K., 2016, '3D scaffold alters cellular response to graphene in a polymer composite for orthopedic applications', Journal of Biomedical Materials Research Part B: Applied Biomaterials, 104, 732-749.

Kumar, S., Raj, S., Kolanthai, E., Sood, A.K., Sampath, S. & Chatterjee, K., 2015, 'Chemical Functionalization of Graphene To Augment Stem Cell Osteogenesis and Inhibit Biofilm Formation on Polymer Composites for Orthopedic Applications', ACS Applied Materials & Interfaces, 7, 3237-3252.

Kumar, S., Raj, S., Sarkar, K. & Chatterjee, K., 2016, 'Engineering a multi-biofunctional composite using poly(ethylenimine) decorated graphene oxide for bone tissue regeneration', Nanoscale, 8, 6820-6836.

Lacoulonche, F., Gamisans, F., Chauvet, A., Garcia, M.L., Espina, M., & Egea, M.A., 1999, 'Stability and In Vitro Drug Release of Flurbiprofen-Loaded Poly-ε-Caprolactone Nanospheres', Drug Development and Industrial Pharmacy, 25, 9, 983-993.

Leong, K.F., Cheah, C.M. & Chua, C.K., 2003, 'Solid freeform fabrication of three-dimensional scaffolds for engineering replacement tissues and organs', Biomaterials, 24, 2363-2378.

Liu, H., Ding, X., Zhou, G., Li, P., Wei, X. & Fan, Y., 2013, 'Electrospinning of Nanofibers for Tissue Engineering Applications', Journal of Nanomaterials, 495708.

Liu, P., Gong, K., Xiao, P. & Xiao, M., 2000, 'Preparation and characterization of poly(vinyl acetate)-intercalated graphite oxide nanocomposite', Journal of Materials Chemistry, 10, 933-935.

Luo, C.J., Stride, E. & Edirisinghe, M., 2012, 'Mapping the Influence of Solubility and Dielectric Constant on Electrospinning Polycaprolactone Solutions', Macromolecules, 45, 4669-4680.

Ma, P. X., 2004, 'Scaffolds for tissue fabrication', Materials Today, 7, 30-40.

McCullen, S.D., Autefage, H., Callanan, A., Gentleman, E. & Stevens, M.M., 2012, 'Anisotropic Fibrous Scaffolds for Articular Cartilage Regeneration', Tissue Engineering: Part A, 18-20.

Merritt, S.R., Exner, A.A., Lee, Z.H. & Recum, H.A.V., 2012, 'Electrospinning and Imaging', Advanced Engineering Materials, 14, 5, B266-B278.

Murray, E., Thompson, B.C., Sayyar, S. & Wallace, G.G., 2015, 'Enzymatic degradation of graphene/polycaprolactone materials for tissue engineering', Polymer Degradation and Stability, 111, 71-77.

Novoselov, K.S., Geim, A.K., Morozov, S.V., Jiang, D., Zhang, Y., Dubonos, S.V., Grigorieva, I.V. & Firsov, A.A., 2004, 'Electric Field Effect in Atomically Thin Carbon Films', Science, 306, 5696, 666-669.

Okan, B.S., Marset, A., Zanjani, J.S.M., Sut, P.A., Sen, O., Çulha, M. & Menceloglu, Y., 2016, 'Thermally exfoliated graphene oxide reinforced fluorinated pentablock

poly(L-lactide-co-ε-caprolactone) electrospun scaffolds: Insight into antimicrobial activity and biodegradation', Journal of Applied Polymer Science, 43490.

Pitt, C.G., 1990, 'Poly-ε-Caprolactone and Its Copolymers', Biodegradable Polymers as Drug Delivery Systems, 71- 120.

Potts, J.R., Dreyer, D.R., Bielawski, C.W. & Ruoff, R.S., 2011, 'Graphene-based polymer nanocomposites', Polymer, 52, 5-25.

Ramazani, S. & Karimi, M., 2015, 'Aligned poly(ε-caprolactone)/graphene oxide and reduced graphene oxide nanocomposite nanofibers: Morphological, mechanical and structural properties', Materials Science and Engineering: C, 56, 325-334.

Ramazani, S. & Karimi, M., 2016a, 'Study the molecular structure of poly(ε-caprolactone)/graphene oxide and graphene nanocomposite nanofibers', Journal of the Mechanical Behavior of Biomedical Materials, 61, 484-492.

Ramazani, S. & Karimi, M., 2016b, 'Electrospinning of poly(ε-caprolactone) solutions containing graphene oxide: Effects of graphene oxide content and oxidation level', Polymer Composites, 37, 131-140.

Rezwan, K., Chen, Q.Z., Blaker, J.J. & Boccaccini, A.R., 2006, 'Biodegradable and bioactive porous polymer/inorganic composite scaffolds for bone tissue engineering', Biomaterials, 27, 3413-3431.

Rim, N.G., Shin, C.S. & Shin, H., 2013, 'Current approaches to electrospun nanofibers for tissue engineering', Biomedical Materials, 8, 014102.

Sahay, R., Kumar, P.S., Sridhar, R., Sundaramurthy, J., Venugopal, J., Mhaisalkar, S.G. & Ramakrishna, S., 2012, 'Electrospun composite nanofibers and their multifaceted applications', Journal of Materials Chemistry, 22, 12953.

Sayyar, S., Cornock, R., Murray, E., Beirne, S., Officer, D.L. & Wallace, G.G., 2014, 'Extrusion Printed Graphene/Polycaprolactone/Composites for Tissue Engineering', Materials Science Forum, 773-774, 496-502.

Sayyar, S., Murray, E., Thompson, B.C., Gambhir, S., Officer, D.L. & Wallace, G.G., 2013, 'Covalently linked biocompatible graphene/polycaprolactone composites for tissue engineering', Carbon, 52, 296-304.

Shah, S., Yin, P.T., Uehara, T.M., Chueng, S.T.D., Yang, L. & Lee, K.B., 2014, 'Guiding Stem Cell Differentiation into Oligodendrocytes Using Graphene-Nanofiber Hybrid Scaffolds', Advanced Materials, 26, 3673-3680.

Shen, H., Zhang, L., Liu, M. & Zhang, Z., 2012, 'Biomedical Applications of Graphene', Theranostics, 2, 3, 283-294.

Sill, T.J. & Recum, H.A.V., 2008, 'Electrospinning: Applications in drug delivery and tissue engineering', Biomaterials, 29, 1989-2006.

Song, J., Gao, H., Zhu, G., Cao, X., Shi, X. & Wang, Y., 2015, 'The preparation and characterization of polycaprolactone/graphene oxide biocomposite nanofiber scaffolds and their application for directing cell behaviors', Carbon, 95, 1039-1050.

Sravanthi, R., 2009, 'Preparation and characterization of poly (ε-caprolactone) PCL scaffolds for tissue engineering applications', Master of Technology Thesis, Department of Biotechnology and Medical Engineering, National Institute of Technology Rourkela.

Thinh, P.X., Basavajara, C., Kim, I.K. & Huh, D.S., 2012, 'Characterization and electrical properties of honeycomb-patterned poly(ε-caprolactone)/reduced graphene oxide composite film', Polymer Composites, 33, 2159-2168.

Thinh, P.X., Basavajara, C., Kim, I.K. & Huh, D.S., 2013, 'Fabrication and characterization of honeycomb-patterned film from poly(ε-caprolactone)/poly((R)-3-hydroxybutyric acid)/reduced graphene oxide composite', Polymer Journal, 1-8.

Uehara, T.M., 2014, 'Interaction of nanomaterials with cell membrane models and with neural stem cells', Tese, Escola de Engenharia de São Carlos, Universidade de São Paulo.

Wan, C. & Chen, B., 2011, 'Poly(ε-caprolactone)/graphene oxide biocomposites: mechanical properties and bioactivity', Biomedical Materials, 6, 055010.

Wan, C. & Chen, B., 2012, 'Reinforcement and interphase of polymer/graphene oxide nanocomposites', Journal of Materials Chemistry, 22, 3637.

Wang, B., Li, Y., Weng, G., Jiang, Z., Chen, P., Wang, Z. & Gu, Q., 2014, 'Reduced graphene oxide enhances the crystallization and orientation of poly(ε-caprolactone)', Composites Science and Technology, 96, 63-70.

Wang, B., Zhang, Y., Zhang, J., Li, H., Chen, P., Wang, Z. & Gu, Q., 2013, 'Noncovalent Method for Improving the Interaction between Reduced Graphene Oxide and Poly(ε-caprolactone)', Industrial & Engineering Chemistry Research, 52, 15824-15828.

Wang, G., Yang, S., Wei, Z., Dong, X., Wang, H. & Qi, M., 2013, 'Facile preparation of poly(ε-caprolactone)/Fe_3O_4@graphene oxide superparamagnetic nanocomposites', Polymer Bulletin, 70, 2359-2371.

Wang, G., Wei, Z.Y., Sang, L., Chen, G.Y., Zhang, W.X., Dong, X.F. & Qi, M., 2013, 'Morphology, crystallization and mechanical properties of poly(ε-caprolactone)/graphene oxide nanocomposites', Chinese Journal of Polymer Science, 31, 1148-1160.

Wang, R., Wang, X., Chen, S. & Jiang, G., 2012, 'In Situ Polymerization Approach to Poly(ε-caprolactone)-Graphene Oxide Composites', Designed Monomers & Polymers, 15, 303-310.

Wang, X., Hu, Y.A., Song, L., Yang, H.Y., Xing, W.Y. & Lu, H.D., 2011, 'In situ polymerization of graphene nanosheets and polyurethane with enhanced mechanical and thermal properties', Journal of Materials Chemistry, 21, 4222-4227.

Woodruff, M.A. & Hutmacher, D.W., 2010, 'The return of a forgotten polymer : Polycaprolactone in the 21st century', Progress in Polymer Science, 35, 10, 1217-1256.

Yi, D.H., Yoo, H.J. & Cho, J.W., 2015, 'Mechanical and photothermal shape memory properties of in-situ polymerized hyperbranched polyurethane composites with functionalized graphene', Fibers and Polymers, 16, 1766-1771.

Yoo, H.J., Mahapatra, S.S. & Cho, J.W., 2014, 'High-Speed Actuation and Mechanical Properties of Graphene-Incorporated Shape Memory Polyurethane Nanofibers', The Journal of Physical Chemistry C, 118, 10408-10415.

You, Y., Min, B.M., Lee, S.J., Lee, T.S. & Park, W.H., 2005, ' In vitro degradation behavior of electrospun polyglycolide, polylactide, and poly(lactide-co-glycolide)', Journal of Applied Polymer Science, 95, 193-200.

Yu, T., Wang, G., Liu, L., Wang, P., Wei, Z. & Qi, M., 2012, 'Synthesis of PCL / Graphene Oxide Composites by In Situ Polymerization', Advanced Materials Research, 518-523, 837-840.

Zhang, J. & Qiu, Z., 2011, 'Morphology, Crystallization Behavior, and Dynamic Mechanical Properties of Biodegradable Poly(ε-caprolactone)/Thermally Reduced Graphene Nanocomposites', Industrial & Engineering Chemistry Research, 50, 13885-13891.